Image features from morphological scale-spaces

Sébastien Lefèvre
LSIIT, University Strasbourg I — CNRS
Pôle API, Bd Brant, 67412 Illkirch, France
lefevre@lsiit.u-strasbg.fr

Abstract

Multimedia data mining is a critical problem due to the huge amount of data available. Efficient and reliable data mining solutions requires both appropriate features to be extracted from the data and relevant techniques to cluster and index the data. In this chapter, we deal with the first problem which is feature extraction for image representation. A wide range of features has been introduced in the literature, and some attempts have been made to build standards (e.g. MPEG-7). These features are extracted with image processing techniques, and we focus here on a particular image processing toolbox, namely the mathematical morphology, which stays rather unknown from the multimedia mining community, even if it offers some very interesting feature extraction methods. We review here these morphological features, from the basic ones (granulometry or pattern spectrum, differential morphological profile) to more complex ones which manage to gather complementary information.

Keywords: Mathematical morphology, Image representation, Local features, Global features, Multidimensional features, Scale-space.

Introduction

With the growth of multimedia data available on personal storage or on the Internet, the need for robust and reliable data mining techniques becomes more necessary than ever. In order these techniques to be really useful with multimedia data, the features used for data representation should be chosen attentively and accurately depending on the data considered: images, video sequences, audio files, 3-D models, web pages, etc.

As features are of primary importance in the process of multimedia mining, a wide range of features has been introduced in particular since the last decade. Some attempts have been made to gather the most relevant and robust features into commonly adopted standards, such as MPEG-7 [67]. For the description of still images, MPEG-7 contains an heterogeneous but complementary set of descriptors which are related to various properties (e.g. colour, texture, 2-D shape, etc).

In addition to well-known standards such as MPEG-7, local or global descriptions of digital images can be achieved through the use of various toolboxes from the image analysis and processing field. Among these toolboxes, Mathematical Morphology offers a robust theoretical framework and a set of efficient tools to describe and analyse images. We believe it can be a very relevant solution for image representation in the context of multimedia mining. Indeed, its nonlinear behaviour comes with several attractive properties, such as translation invariance (both in spatial and intensity domains) and other properties (e.g. idempotence, extensivity or anti-extensivity, increasingness, connectedness, duality and complementariness, etc), depending on the morphological operator under consideration. Moreover, it allows very easily the construction of image scale-spaces from which can be extracted some robust features.

The goal of this chapter is not to present once again a well-known standard such as MPEG-7 but rather to focus on a specific theory, namely the Mathematical Morphology, and to review how the tools it offers can be used to generate global or local features for image representation. This chapter is organised as follows. First we recall the foundations of Mathematical Morphology and give the necessary definitions and notations. Then we present the morphological one-dimensional features which can be

computed from the images either at a local or a global scale but always from a scale-space analysis of the images. In a third section we review several extensions which have been proposed to gather more information than these standard features through multidimensional morphological features. Next we focus on the implementation aspects, and give indications on the available methods for efficient processing, which is needed as soon as these features are used with multimedia indexing. We underline the potential of these features in a following section by giving a brief survey of their use in various application fields. Finally we give some concluding remarks and suggest further readings related to the topic addressed in this chapter.

1 Basics of Mathematical Morphology

Mathematical Morphology is a theory introduced about 50 years ago by Georges Matheron and Jean Serra. Since then, it has been a growing and very active field of research, with its regular International Symposium on Mathematical Morphology (ISMM) taking place every two years and a half, and several recent special issues of journals [92, 93].

1.1 Theoretical foundations

Basically, Mathematical Morphology relies on the spatial analysis of images through a pattern called structuring element (SE) and consists in a set of nonlinear operators which are applied on the images considering this SE. Thus it can be seen as a relevant alternative to other image processing techniques such as purely statistical approaches or linear approaches. First works in Mathematical Morphology were related to binary image processing. The theoretical framework involved initially was very logically the set theory. Within this framework, the morphological operators were defined by means of set operators such as inclusion, union, intersection, difference, etc. However, despite initial efforts leading to stack approaches, this theory has been shown insufficient as soon as more complex images such as greyscale images were considered. So another theoretical framework, namely the (complete) lattice theory, is now widely considered as appropriate to define morphological operators [91].

In order to define the main morphological operators from the lattice theory viewpoint, let us note $f : E \rightarrow T$ a digital image, where E is the discrete coordinate grid (usually $\mathbb{N}^2$ for a 2-D image, or $\mathbb{N}^3$ for a 3-D image or a 2-D+t image sequence) and T is the set of possible image values. In the case of a binary image, $T = \{0, 1\}$ where the objects and the background are respectively represented by values equal to 1 and 0. In the case of a greyscale image, T can be defined on $\mathbb{R}$, but it is often defined rather on a subset of $\mathbb{Z}$, most commonly $[0, 255]$. In case of multidimensional images such as colour images, multispectral or multimodal images, T is defined on $\mathbb{R}^n$ or $\mathbb{Z}^n$, with n the number of image channels.

A complete lattice is defined from three elements:

- a partially ordered set $(T, \geq)$, which could be the set inclusion order for binary images, the natural order of scalars for greyscale images, etc,
- an infimum or greatest lower bound $\wedge$, which is most often computed as the minimum operator (this choice will also be made here for the sake of simplicity),
- a supremum or least upper bound $\vee$, which is similarly most often computed as the maximum operator.

Once a complete lattice structure has been imposed on the image data, it is possible to apply morphological operators using a structuring pattern. It is called structuring function (SF) or functional structuring element and noted g when defined as a function on a subset of T, and called structuring element (SE) and noted b when defined as a set on E. In this chapter and for the sake of simplicity, we will assume the latter case unless otherwise mentioned, and use the so-called flat structuring elements. Let us notice however that the features reviewed in this chapter can easily be computed with structuring functions without important modification (if any).

1.2 Erosion and dilation

From these theoretical requirements, one can define the two basic morphological operators. The first one called *erosion* is defined as:

$$\varepsilon_b(f)(p) = \bigwedge_{q \in b} f(p+q), \;\; p \in E \tag{1.1}$$

where p is the pixel coordinates, e.g. $p = (x, y)$ in 2-D images or $p = (x, y, z)$ in 3-D images. The coordinates within the SE b are denoted by q and most commonly defined in the same space as p. In binary images, erosion will reduce white areas (or enlarge black areas). In greyscale or more complex images, it will spread the lowest pixel values (i.e. the darkest pixels in case of greyscale images) while removing the highest ones (i.e. the brightest pixels in case of greyscale images). In other words, the erosion results in an image where each pixel p is associated with the local minimum of f computed in the neighbourhood defined by the SE b.

The other main morphological operator is called *dilation* and is defined in a dual way as:

$$\delta_b(f)(p) = \bigvee_{q \in \check{b}} f(p+q), \;\; p \in E \tag{1.2}$$

Here the result is an image where each pixel p is associated to the local maximum of f in the neighbourhood defined by the SE b. Thus it will enlarge areas with highest values (i.e. brightest pixels) while reducing areas with lowest values (i.e. darkest pixels). Another main difference is related to the SE: contrary to the erosion where b is considered, here the dilation is applied using the transposed SE $\check{b} = \{-q \mid q \in b\}$. In other words, the dilation can be defined as:

$$\delta_b(f)(p) = \bigvee_{q \in b} f(p-q), \;\; p \in E \tag{1.3}$$

Mathematical morphology is of particular interest due to the numerous properties verified by its operators. Indeed, morphological operators such as erosion and dilation (but also the more complex ones) are invariant to (spatial and greyscale) translations, commutative, associative, increasing, distributive, dual with respect to the complementation, and can most often be broken down into simple operators.

Erosion and dilation, as many other morphological operators, require the definition of a structuring element b. This parameter has a strong impact on the results returned by an operator. Main SE shapes are diamond ♦, square ■, cross $+$, disc •, and line $-$ or $|$. A pixel and its 4- or 8-neighbourhood correspond respectively to a 3×3 pixel diamond- or square-shaped SE, also called elementary isotropic (or symmetric) SE. The shape of the SE can also be defined from a basic shape and an homothetic parameter (or SE size), so we will use the notation $b_\lambda = \lambda b$ to represent a SE of shape b and size λ. For most of the SE shapes, b_λ can be generated from $\lambda - 1$ successive dilations, i.e. $b_\lambda = \delta_{\check{b}}^{(\lambda-1)}(b)$. This is obviously not true with disc-shaped SE, where $\bullet_\lambda = \{p : d(p, o) \leq \lambda\}$ with o the origin or centre of the disc, and d the exact or approximated Euclidean distance. Moreover, we can also consider a growing factor κ between successive λ sizes, i.e. $b_\lambda = \kappa\lambda b$. For the sake of simplicity, the b parameter may be omitted in formulas, e.g. $\varepsilon_\lambda = \varepsilon_{b_\lambda}$ and $\delta_\lambda = \delta_{b_\lambda}$. For elementary structuring elements (e.g. $\blacksquare_1$ or $\blacklozenge_1$), we may also omit the $\lambda = 1$ parameter, i.e. $\varepsilon = \varepsilon_1$ and $\delta = \delta_1$, thus resulting in elementary erosion an dilation. We also state that $\varepsilon_0(f) = \delta_0(f) = f$. Fig. 1 illustrates the basic structuring elements used in mathematical morphology.

Since morphological operators are often applied several times successively, we will use the notation $\varepsilon^{(n)}(f)$ and $\delta^{(n)}(f)$ to denote respectively the n successive applications of ε and δ on f. In other words, $\varepsilon^{(n)}(f) = \varepsilon^{(1)}(\varepsilon^{(n-1)}(f))$ and $\delta^{(n)}(f) = \delta^{(1)}(\delta^{(n-1)}(f))$, with $\varepsilon^{(1)} = \varepsilon$ and $\delta^{(1)} = \delta$.

Even if most of the features presented in this chapter will be defined with flat SE b (i.e. sets), they can easily be defined also with structuring functions (SF) g. In this case, the basic operations are defined as:

$$\varepsilon_g(f)(p) = \bigwedge_{q \in \mathrm{supp}(g)} f(p+q) - g(q), \;\; p \in E \tag{1.4}$$

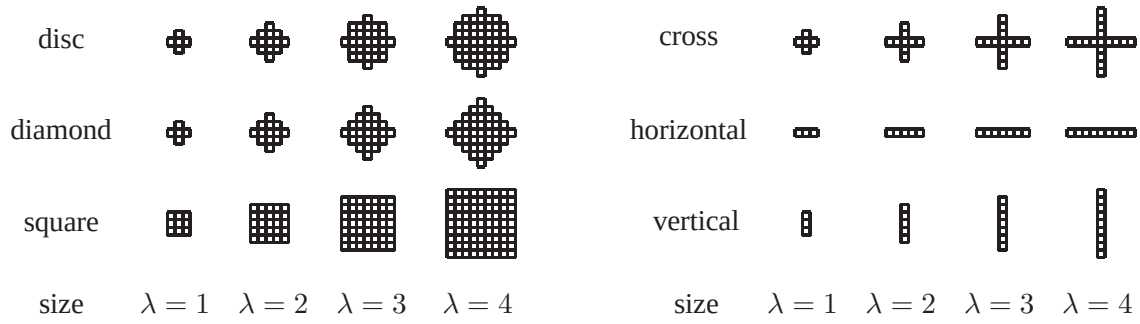

Figure 1: Illustrative examples of basic SE with increasing size λ.

and

$$\delta_g(f)(p) = \bigvee_{q \in \mathrm{supp}(g)} f(p-q) + g(q), \;\; p \in E \tag{1.5}$$

with $\mathrm{supp}(g)$ representing the support of g, i.e. the points for which the SF is defined.

Fig. 2 and 3 illustrate the effects of morphological erosions and dilations applied respectively on binary and greyscale images with 8-connected elementary SE $\blacksquare_\lambda$ of increasing size.

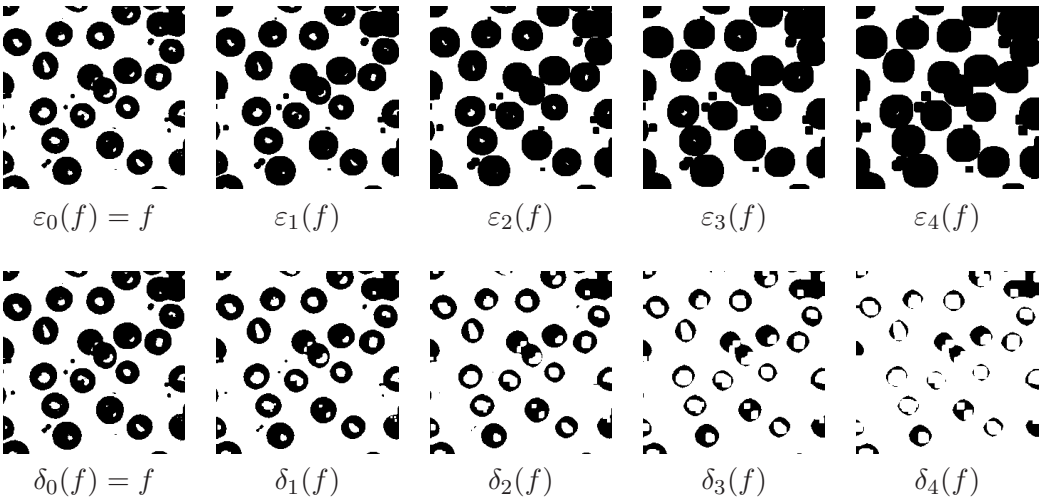

Figure 2: Binary erosion and dilation with square-shaped SE $\blacksquare_\lambda$ of increasing size λ.

1.3 Opening and closing

These two operators are used to build most of the other morphological operators. Among these operators, we can mention the well-known *opening* and *closing* filters where erosion and dilation are applied successively to filter the input image, starting with erosion for the opening and with dilation for the closing. Opening is defined by

$$\gamma_b(f) = \delta_{\check{b}}(\varepsilon_b(f)) \tag{1.6}$$

while closing is defined by

$$\varphi_b(f) = \varepsilon_{\check{b}}(\delta_b(f)) \tag{1.7}$$

These two operators respectively result in a removal of local maxima or minima and return filtered images which are respectively lower and higher than the input image. This is called the extensivity property of the opening with $\gamma(f) \leq f$ and the anti-extensivity property of the closing with $f \leq \varphi(f)$ (with the $\leq$ relation being replaced by the $\subseteq$ relation if set theory is considered). Moreover, both opening and closing share some very nice properties (in addition to those of erosion and dilation). First the have the

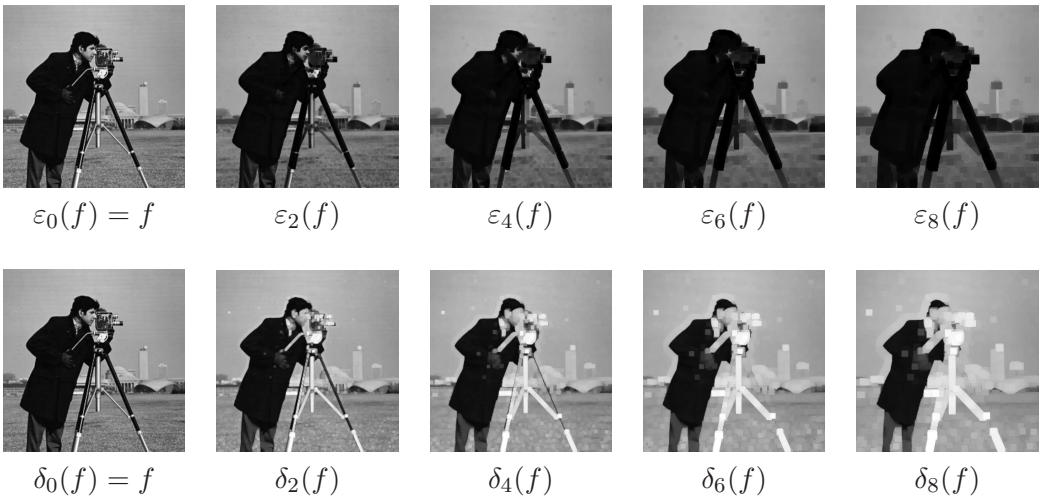

Figure 3: Greyscale erosion and dilation with square-shaped SE $\blacksquare_\lambda$ of increasing size λ.

idempotence property since $\gamma_b(\gamma_b(f)) = \gamma_b(f)$ and $\varphi_b(\varphi_b(f)) = \varphi_b(f)$. Second they also ensure the increasing property, i.e. if $f \leq g,\ \gamma_b(f) \leq \gamma_b(g)$ and $\varphi_b(f) \leq \varphi_b(g)$. Since they verify these two properties, they are called morphological filters.

Fig. 4 and 5 illustrate the effects of morphological openings and closings applied respectively on binary and greyscale images with 8-connected elementary SE $\blacksquare_\lambda$ of increasing size.

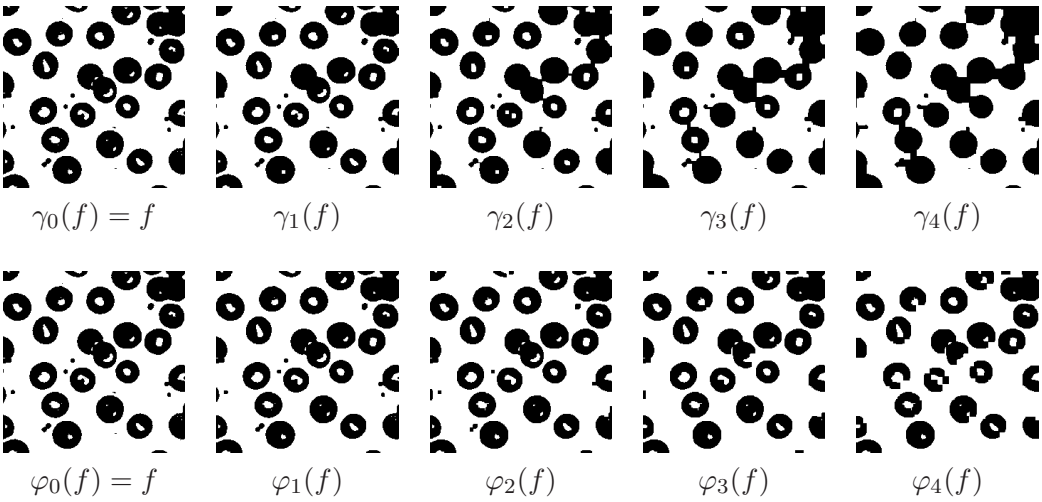

Figure 4: Binary opening and closing with square-shaped SE $\blacksquare_\lambda$ of increasing size λ.

The main concern with these two morphological filters is their very strong sensitivity to the SE shape, which will have a straight influence on the shapes visible in the filtered image. In order to avoid this problem, it is possible to involve the so-called algebraic filters which are a generalisation of the morphological opening and closing defined above. For the sake of conciseness, we will use in this chapter the operator ψ to represent any morphological filter (e.g. γ or φ).

1.4 Algebraic filters

The term algebraic opening (respectively closing) is related to any transformation which is increasing, anti-extensive (respectively extensive) and idempotent. Thus morphological (also called structural) opening and closing are a particular case of algebraic filters. The two main ways of creating algebraic opening and closing are recalled here.

The first option relies on opening and closing by reconstruction, which are useful to preserve original object edges. More precisely, let us note $\varepsilon_g^{(1)}(f)$ the geodesic erosion of size 1 of the marker image f

$\gamma_0(f) = f$ $\gamma_2(f)$ $\gamma_4(f)$ $\gamma_6(f)$ $\gamma_8(f)$

$\varphi_0(f) = f$ $\varphi_2(f)$ $\varphi_4(f)$ $\varphi_6(f)$ $\varphi_8(f)$

Figure 5: Greyscale opening and closing with square-shaped SE $\blacksquare_\lambda$ of increasing size λ.

with respect to the mask image g:

$$\varepsilon_g^{(1)}(f)(p) = \varepsilon^{(1)}(f)(p) \vee g(p) \tag{1.8}$$

where the elementary erosion is limited (through a lower bound) within the mask, i.e. $\varepsilon_g \geq \varepsilon$.

Similarly, the geodesic dilation of size 1 is defined by:

$$\delta_g^{(1)}(f)(p) = \delta^{(1)}(f)(p) \wedge g(p) \tag{1.9}$$

where the elementary dilation is limited (through an upper bound) within the mask, i.e. $\delta_g \leq \delta$.

These two operators are usually applied several times iteratively, thus we will use the following notations:

$$\varepsilon_g^{(n)}(f) = \varepsilon_g^{(1)}(\varepsilon_g^{(n-1)}(f)) \tag{1.10}$$

and

$$\delta_g^{(n)}(f) = \delta_g^{(1)}(\delta_g^{(n-1)}(f)) \tag{1.11}$$

From these two geodesic operators, it is possible to build reconstruction filters ρ which consists in successive applications of these operators until convergence. More precisely, the morphological reconstruction by erosion and by dilation are respectively defined by:

$$\rho_g^{\varepsilon}(f) = \varepsilon_g^{(j)}(f) \text{ with } j \text{ such as } \varepsilon_g^{(j)}(f) = \varepsilon_g^{(j-1)}(f) \tag{1.12}$$

and

$$\rho_g^{\delta}(f) = \delta_g^{(j)}(f) \text{ with } j \text{ such as } \delta_g^{(j)}(f) = \delta_g^{(j-1)}(f) \tag{1.13}$$

Based on these reconstruction filters, new morphological filters which preserve object edges can be defined. Indeed, the opening by reconstruction $\gamma_b^{\rho}(f)$ of the image f using the SE b is defined as:

$$\gamma_b^{\rho}(f) = \rho_f^{\delta}(\varepsilon_b(f)) \tag{1.14}$$

while the closing by reconstruction $\varphi_b^{\rho}(f)$ is defined by:

$$\varphi_b^{\rho}(f) = \rho_f^{\varepsilon}(\delta_b(f)) \tag{1.15}$$

In other words, for the opening (resp. closing) by reconstruction, the image f is used both as input for the first erosion (resp. dilation) and as mask for the following iterative geodesic dilations (resp. erosions). Contrary to their standard counterparts, these morphological filters by reconstruction remove details without modifying the structure of remaining objects.

The second option consists in computing various openings (respectively closings) and select their supremum (respectively infimum). Here each opening is related to a different condition or SE. Let us consider a set $B = (b)_i$ of SE, we can then define respectively the algebraic openings and closings by:

$$\gamma_B^\alpha(f) = \bigvee_{b \in B} \gamma_b(f) \tag{1.16}$$

and

$$\varphi_B^\alpha(f) = \bigwedge_{b \in B} \varphi_b(f) \tag{1.17}$$

and we will use the shortcuts $\gamma_\lambda^\alpha = \gamma_{\lambda B}^\alpha$ and $\varphi_\lambda^\alpha = \varphi_{\lambda B}^\alpha$ with $\lambda B = (\lambda b)_i$.

Among the main algebraic filters, we can mention the area-based operators, which have the very interesting property to be invariant to the shape of the SE b under consideration. To do so, they consider the whole set of all SE of a given size λ, thus resulting in the following operators:

$$\gamma_\lambda^a(f) = \bigvee_b \{\gamma_b(f) \mid b \text{ is connected and } \mathrm{card}(b) = \lambda\} \tag{1.18}$$

and

$$\varphi_\lambda^a(f) = \bigwedge_b \{\varphi_b(f) \mid b \text{ is connected and } \mathrm{card}(b) = \lambda\} \tag{1.19}$$

Area filters ψ^a are a special case of more general attribute filters ψ^χ, with the attribute or criterion χ to be satisfied being related to the area, i.e. the Boolean function $\chi(b, \lambda) = \{\mathrm{card}(b) = \lambda\}$. Other attribute filters can be elaborated, in particular shape-related ones, involving for instance the perimeter $\chi(b, \lambda) = \{\mathrm{card}(b - \varepsilon(b)) = \lambda\}$ or the moment of inertia $\chi(b, \lambda) = \{\sum_{q \in b} d(q, o) = \lambda\}$ (with d the Euclidean distance and o the origin of the SE b). More generally, attribute filters can be defined as:

$$\gamma_\lambda^\chi(f) = \bigvee_b \{\gamma_b(f) \mid b \text{ is connected and } \chi(b, \lambda)\} \tag{1.20}$$

and

$$\varphi_\lambda^\chi(f) = \bigwedge_b \{\varphi_b(f) \mid b \text{ is connected and } \chi(b, \lambda)\} \tag{1.21}$$

In Fig. 6 and 7 are given some visual comparisons between structural filters, filters by reconstruction, and area filters, respectively on binary and greyscale images. We can observe the interest of filters by reconstruction and area filters to limit the sensitivity to the SE shape.

Apart from these basic operators, mathematical morphology offers a wide range of operators or methods to process images. We can cite the morphological gradient, the hit-or-miss transform to perform template matching or object skeletonisation, the watershed or levelling approaches for segmentation, the alternating sequential filters (ASF) for image simplification, etc. In this chapter, we will focus on morphological features extracted from the previously presented operators and we will not deal with some other morphological operators. The interested reader will find in the book from Pierre Soille a good overview of the morphological toolbox for image processing and analysis [104].

2 Standard morphological image features

Image features are most often dedicated to a single type of information (e.g. colour, texture, spatial distribution, shape, etc). The most famous example is undoubtly the histogram which measures the probability density function of the intensity values in the image and which can be analysed through various measures (e.g. moments, entropy, uniformity, etc). However it is limited to intensity distribution and does not take into account the spatial relationships between pixels.

On the opposite, approaches known under the terms of pattern spectra, granulometries, or morphological profiles are built from series of morphological filtering operations and thus involve a spatial information. We review here these different (either global or local) features in an unified presentation.

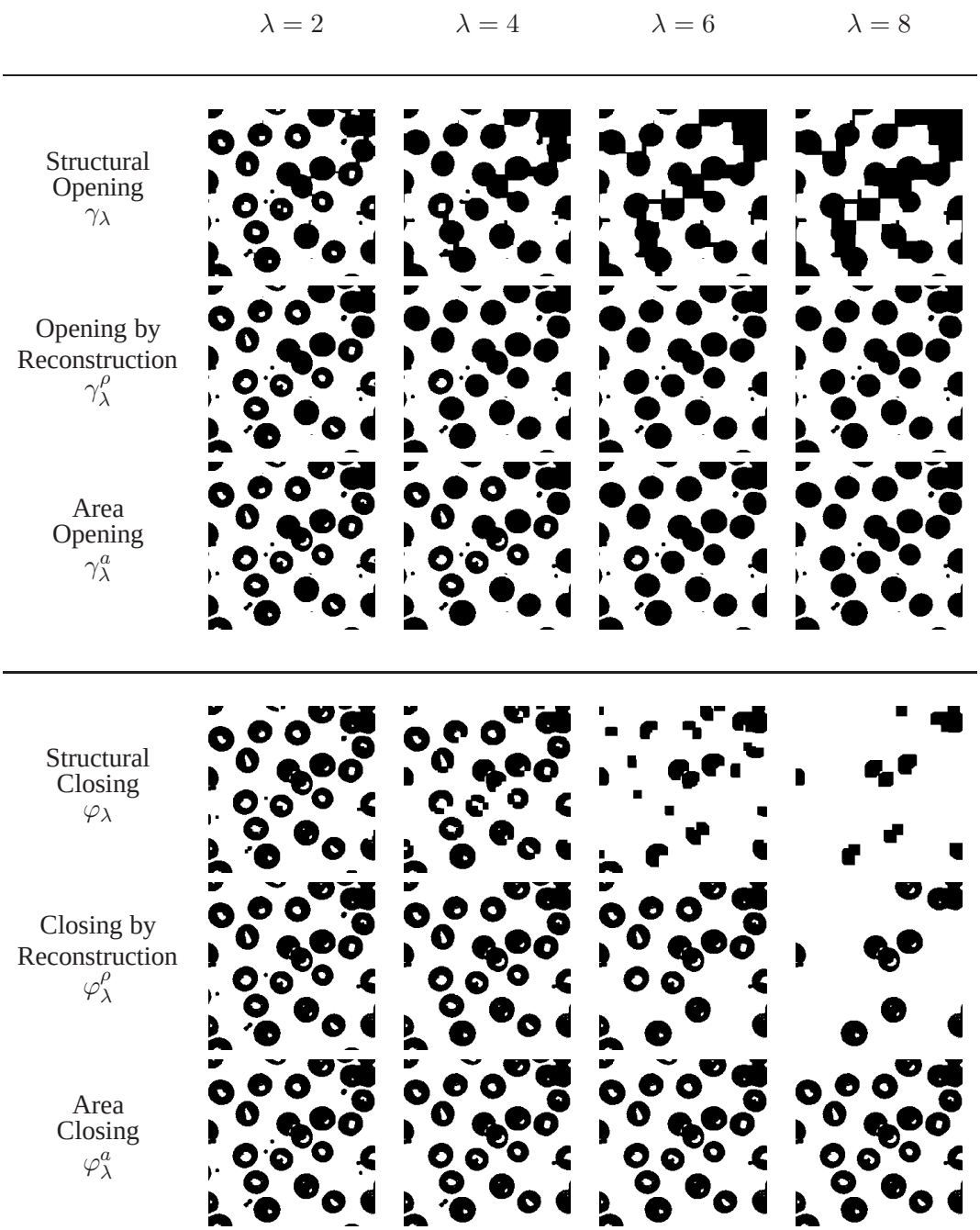

Figure 6: Comparison between binary standard (structural) filters, filters by reconstruction, and area filters with increasing λ parameter.

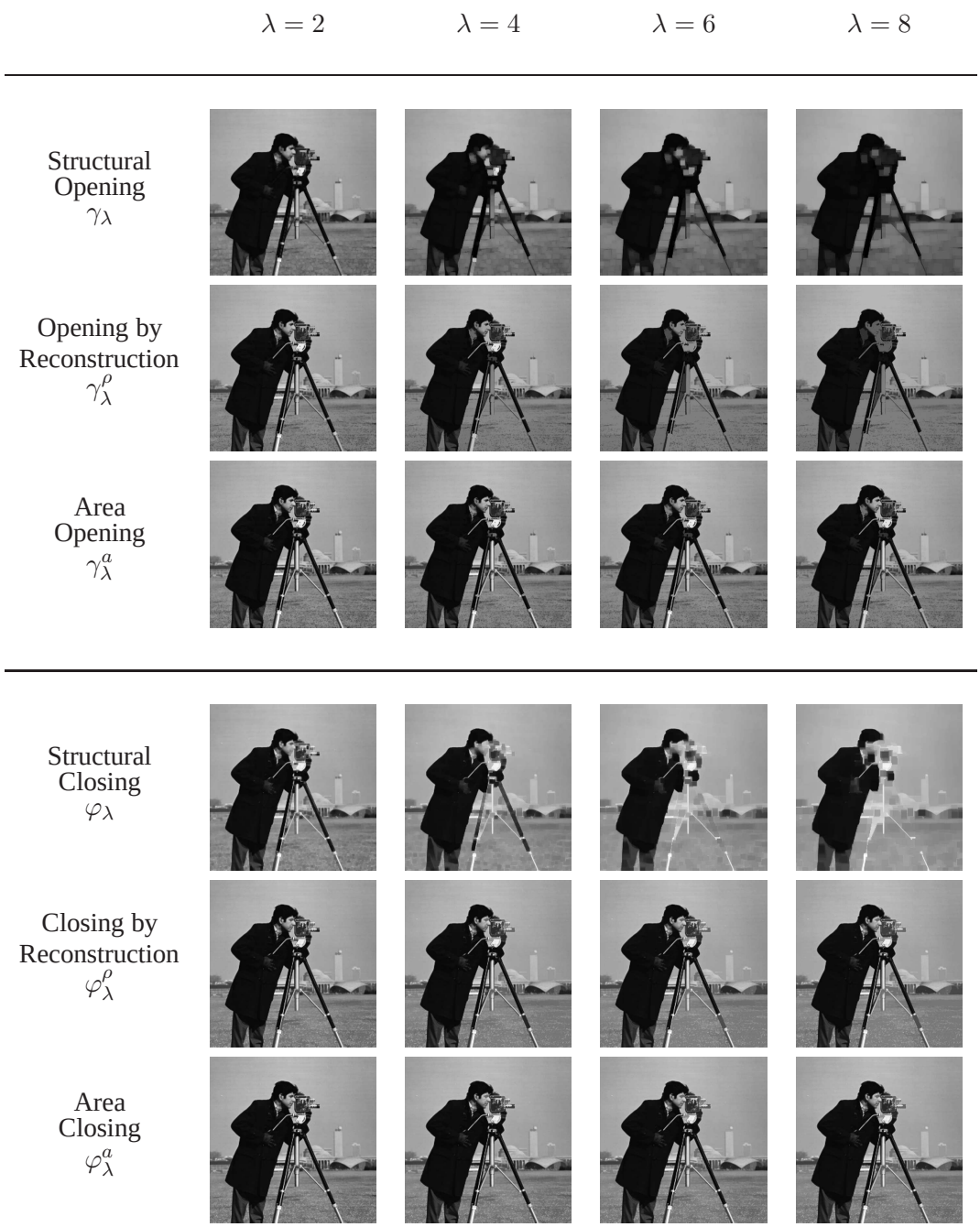

Figure 7: Comparison between greyscale standard (structural) filters, filters by reconstruction, and area filters with increasing λ parameter.

2.1 Multiscale representation using morphological filters

We have introduced in section 1 the main morphological filters (i.e. opening and closing filters) which aim at removing details in the image, either bright details (with the opening) or dark details (with the closing), by preserving or not object edges. Thus they can be used to build multiscale representations of digital images by means of mathematical morphology.

Most of these multiscale representations can be seen as nonlinear scale-spaces, if some of the original constraints are relaxed. The concept of scale space introduced by Witkin [129] is defined as a family of filtered images $\{\Upsilon_t(f)\}_{t\geq 0}$, with $\Upsilon_0(f) = f$ and various axioms [32], the multiscale representation being computed most often by means of a convolution by a Gaussian kernel:

$$\Upsilon_t(f)(x,y) = f(x,y) * g(x,y,t) = \int_{-\infty}^{+\infty} f(u,v)\frac{1}{2\pi t^2}e^{-\frac{(x-u)^2+(y-v)^2}{2t^2}}du\,dv \tag{2.1}$$

The main properties of a scale-space are relatively compatible with some of the morphological operators as pointed out by the work of Jackway [51]:

- causality, i.e. no additional structures are created in the image when t increases (indeed both height and position of extrema are preserved);
- recursivity
$$\Upsilon_t(\Upsilon_s(f)) = \Upsilon_s(\Upsilon_t(f)) = \Upsilon_{t+s}(f),\ \ \forall t,s \geq 0 \tag{2.2}$$
- increasingness
$$f \leq g,\ \ \Upsilon_t(f) < \Upsilon_t(g),\ \ \forall t > 0 \tag{2.3}$$
- either anti-extensivity
$$\Upsilon_t(f) \geq f,\ \ \forall t \geq 0 \tag{2.4}$$
or extensivity
$$\Upsilon_t(f) \leq f,\ \ \forall t \geq 0 \tag{2.5}$$
which leads respectively to
$$t_1 \leq t_2,\quad \Upsilon_{t_1}(f) < \Upsilon_{t_2}(f),\ \ \forall t > 0 \tag{2.6}$$
$$t_1 \leq t_2,\quad \Upsilon_{t_1}(f) > \Upsilon_{t_2}(f),\ \ \forall t > 0 \tag{2.7}$$

Thus some scale-spaces can be built straightforward from successive applications of morphological operators (such as erosion and dilations [52], or ASF [71, 82, 16]), or using advanced morphological representations such as max-tree [97]. Here we will use the term (morphological) scale-space even for scale-spaces where the recursivity property is replaced by the absorption law defined by Matheron in [70] which is relevant for morphological filters:

$$\forall t,s \geq 0,\ \ \Upsilon_t(\Upsilon_s(f)) = \Upsilon_s(\Upsilon_t(f)) = \Upsilon_{\max(t,s)}(f) \tag{2.8}$$

In addition to this property, the idempotence property also holds:

$$\Upsilon_t(\Upsilon_t(f)) = \Upsilon_t(f) \tag{2.9}$$

A wide range of morphological operators can lead to scale spaces, such as openings and closings [27].

Fig 8 illustrates the difference between a scale-space built with Gaussian and morphological closing filters. One can clearly see the interest of morphological scale-spaces to retain object edges even with basic (i.e. structural) morphological filters.

So morphological scale-spaces can be built by applying some morphological operators Υ_t on the input image f, with increasing parameter t. In the morphological framework, t is directly related to the size λ of the structuring element b, and we will use the notation $\Upsilon_\lambda = \Upsilon_{b_\lambda}$. Indeed, for a given morphological filter ψ_λ, λ denotes the size of the SE, i.e. the size of neighbourhood used to compute

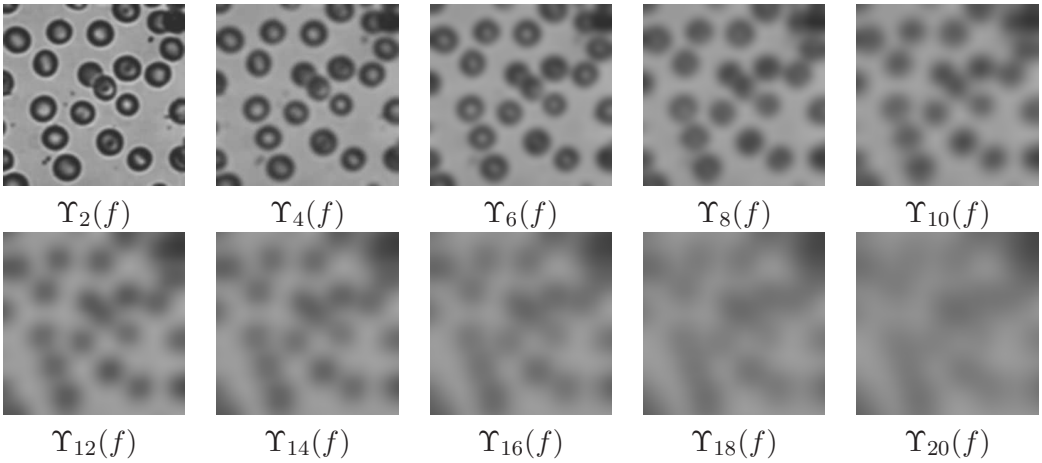

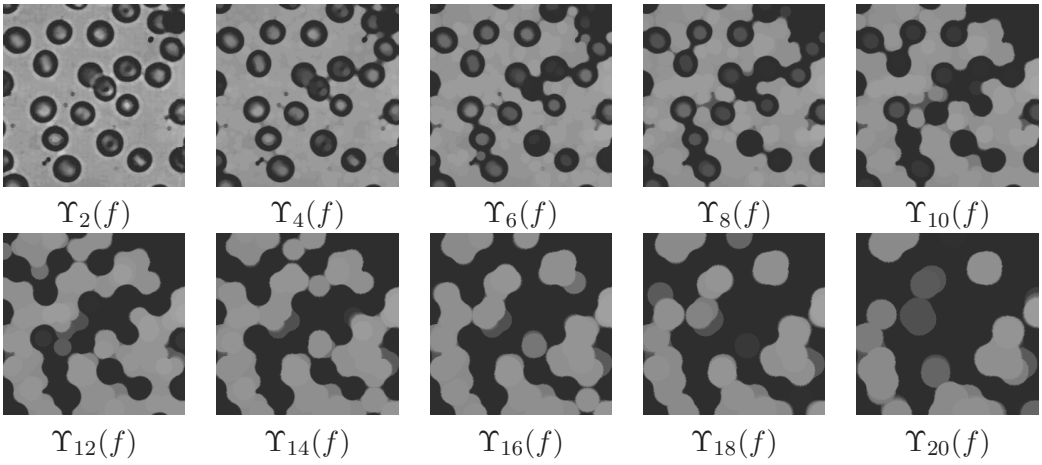

Figure 8: Comparison between Gaussian and Morphological Scale-Spaces.

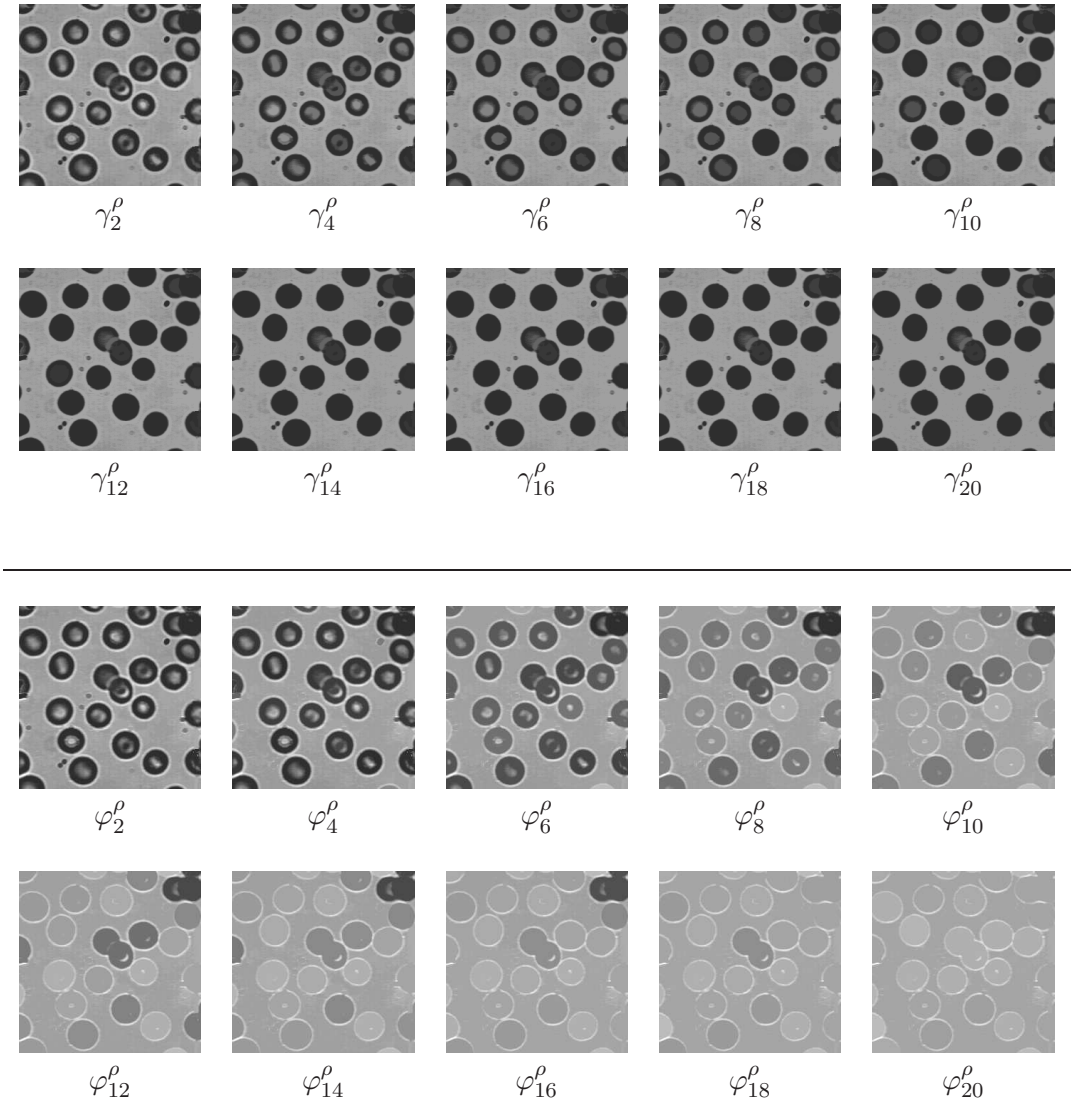

Figure 9: Details removal by means of successive openings and closing by reconstruction.

minima or maxima (or the filter window). Then when λ increases, the morphological filter ψ_λ will remove more and more details from the input image (as shown by Fig. 9), thus respecting the main property of scale-spaces (i.e. causality). Moreover, to satisfy the absorption property, the SE b under consideration has to be a compact convex set [70].

Let us note $\Pi^\psi(f) = \{\Pi^\psi_\lambda(f)\}_{\lambda\geq 0}$ the morphological scale-space, i.e. the series of successive filtered images using ψ with growing SE size λ:

$$\Pi^\psi(f) = \left\{\Pi^\psi_\lambda(f) \mid \Pi^\psi_\lambda(f) = \psi_\lambda(f)\right\}_{0\leq\lambda\leq n} \tag{2.10}$$

where $\psi_0(f) = f$ and $n+1$ is the length of the series (including the original image). This Π series is a nonlinear scale-space, with less and less details as λ is increasing from 0 to n. Instead of using a single SE, a SE set or generator $B = (b)_i$ can be used [70], thus resulting in series made from algebraic filters:

$$\Pi^{\psi^\alpha}(f) = \left\{\Pi^{\psi^\alpha}_\lambda(f) \mid \Pi^{\psi^\alpha}_\lambda(f) = \psi^\alpha_\lambda(f)\right\}_{0\leq\lambda\leq n} \tag{2.11}$$

with $\psi^\alpha_\lambda = \psi^\alpha_{\lambda B}$. The initial definition leading to Euclidean granulometries was considering the same growing factor κ for all SE b_i in B, i.e. $(b_i)_\lambda = \lambda\kappa b_i$. It is also possible to make the κ factor depends on b, thus either $B = (b,\kappa)_i$ (where $(b_i)_\lambda = \lambda\kappa_i b_i$) for homogeneous multivariate series [18] or $B = (b,t,\kappa)_i$ (with t_i being a strictly increasing function of κ_i, thus $(b_i)_\lambda = \lambda t_i(\kappa_i) b_i$) for heterogeneous multivariate series [19].

Figure 10: From top left to bottom right, Π series of length $2n+1$ with $n = 7$ using structural filters γ and φ and 4-connected elementary SE ♦.

Moreover, these series Π^ψ can be made using any ψ filter (see [104] for a deeper review of morphological filters). Thus, Π is also extensive for any opening filter and anti-extensive for any closing filter, resulting respectively in lower and lower images or higher and higher images as λ increases. Indeed, if we have $\lambda_2 \leq \lambda_1$, then $\Pi^\gamma_{\lambda_2}(f) \leq \Pi^\gamma_{\lambda_1}(f)$ and $\Pi^\varphi_{\lambda_2}(f) \geq \Pi^\varphi_{\lambda_1}(f)$.

In order to avoid their highly asymmetric behaviour (Π^ψ is either anti-extensive or extensive), it is possible to gather opening and closing series to generate a single Π series of length $2n+1$:

$$\Pi(f) = \left\{\Pi_\lambda(f) \mid \Pi_\lambda(f) = \begin{cases}\Pi^\gamma_{-\lambda}(f), & \lambda < 0\\ \Pi^\varphi_\lambda(f), & \lambda > 0\\ f, & \lambda = 0\end{cases}\right\}_{-n\leq\lambda\leq n} \tag{2.12}$$

We can also build these symmetric series using any of the pair of opening/closing filters, and we will denote by Π^{ρ}, Π^{α}, Π^{a}, Π^{χ} the series created respectively with ψ^{ρ}, ψ^{α}, ψ^{a}, ψ^{χ}. An illustration of this kind of dual series is given in Fig. 10.

Let us note that the merging of openings and closings can also be made by means of alternate sequential filters (ASF), which consists in successive openings and closing with SE of increasing size λ. Using ASF to compute the Π series results in the following definition:

$$\Pi^{\text{ASF}}(f) = \left\{ \Pi^{\text{ASF}}_{\lambda}(f) \mid \Pi^{\text{ASF}}_{\lambda}(f) = \begin{cases} \gamma_{\lceil \lambda/2 \rceil}(\Pi^{\text{ASF}}_{\lambda-1}(f)) & \text{if } \lambda \text{ is odd} \\ \varphi_{\lceil (\lambda-1)/2 \rceil}(\Pi^{\text{ASF}}_{\lambda-1}(f)) & \text{if } \lambda \text{ is even} \\ f, & \text{if } \lambda = 0 \end{cases} \right\}_{0 \leq \lambda \leq n} \tag{2.13}$$

Of course the morphological filters γ and φ can again be replaced by any of their variants, e.g. their reconstruction-based counterparts γ^{ρ} and φ^{ρ}, thus resulting in the $\Pi^{\text{ASF}^{\rho}}$ series. ASF have been proven to be a specific case of more general concepts, M- and N- sieves [16]. Another related feature is the lomo filter [23], which consists in the mean of two ASF applied until convergence, one starting with an opening (i.e. being defined as $\varphi_n \gamma_n \ldots \varphi_1 \gamma_1$) and the other starting with a closing operation (i.e. being defined as $\gamma_n \varphi_n \ldots \gamma_1 \varphi_1$). It is also possible to associate to each scale λ the difference between the union and the intersection of the ASF with successive λ size [130], i.e. $(\Pi^{\text{ASF}}_{\lambda} \vee \Pi^{\text{ASF}}_{\lambda-1}) - (\Pi^{\text{ASF}}_{\lambda} \wedge \Pi^{\text{ASF}}_{\lambda-1})$.

Features can be extracted directly from the series Π^{ψ} (or from their symmetrical version Π), but most often it is more relevant to compute the differential version Δ^{ψ} of this series where removed details are emphasised for each λ size. For extensive filters such as openings, we have:

$$\Delta^{\gamma}(f) = \left\{ \Delta^{\gamma}_{\lambda}(f) \mid \Delta^{\gamma}_{\lambda}(f) = \Pi^{\gamma}_{\lambda-1}(f) - \Pi^{\gamma}_{\lambda}(f) \right\}_{0 \leq \lambda \leq n} \tag{2.14}$$

while for anti-extensive filters such as closings, we have:

$$\Delta^{\varphi}(f) = \left\{ \Delta^{\varphi}_{\lambda}(f) \mid \Delta^{\varphi}_{\lambda}(f) = \Pi^{\varphi}_{\lambda}(f) - \Pi^{\varphi}_{\lambda-1}(f) \right\}_{0 \leq \lambda \leq n} \tag{2.15}$$

thus resulting in a single definition

$$\Delta^{\psi}(f) = \left\{ \Delta^{\psi}_{\lambda}(f) \mid \Delta^{\psi}_{\lambda}(f) = \left| \Pi^{\psi}_{\lambda}(f) - \Pi^{\psi}_{\lambda-1}(f) \right| \right\}_{0 \leq \lambda \leq n} \tag{2.16}$$

with the assumption $\Delta^{\psi}_{0} = 0$. In this series, a pixel p will appear (i.e. have a non null value) in $\Delta^{\psi}_{\lambda}(f)$ if it is removed by ψ_{λ}, the morphological filter ψ of size λ (or in other words, if it was present in $\psi_{\lambda-1}(f)$ but not anymore in $\psi_{\lambda}(f)$).

Similarly for the Π^{ψ} series, it is possible to compute a symmetric version of Δ^{ψ} by taking into account both opening and closing filters:

$$\Delta(f) = \left\{ \Delta_{\lambda}(f) \mid \Delta_{\lambda}(f) = \begin{cases} \Delta^{\gamma}_{-\lambda}(f), & \lambda < 0 \\ \Delta^{\varphi}_{\lambda}(f), & \lambda > 0 \\ 0, & \lambda = 0 \end{cases} \right\}_{-n \leq \lambda \leq n} \tag{2.17}$$

As an illustration, Fig. 11 is the Δ counterpart of the Π series presented in Fig. 10 using structural filters with diamond shaped-SE, while Fig. 12 is the differential series built from the one presented in Fig. 9 using filters by reconstruction.

We also have to notice that even basic operators (not necessarily filters) can be used to build morphological series. Indeed, one can apply successive erosions ε or dilations δ to build a Π or Δ series:

$$\Pi^{\nu}(f) = \left\{ \Pi^{\nu}_{\lambda}(f) \mid \Pi^{\nu}_{\lambda}(f) = \nu_{\lambda}(f) \right\}_{0 \leq \lambda \leq n} \tag{2.18}$$

where ν denotes the basic morphological operator under consideration (e.g. ε or δ). The properties of these series will be however weaker than the previous series built from morphological filters. Depending

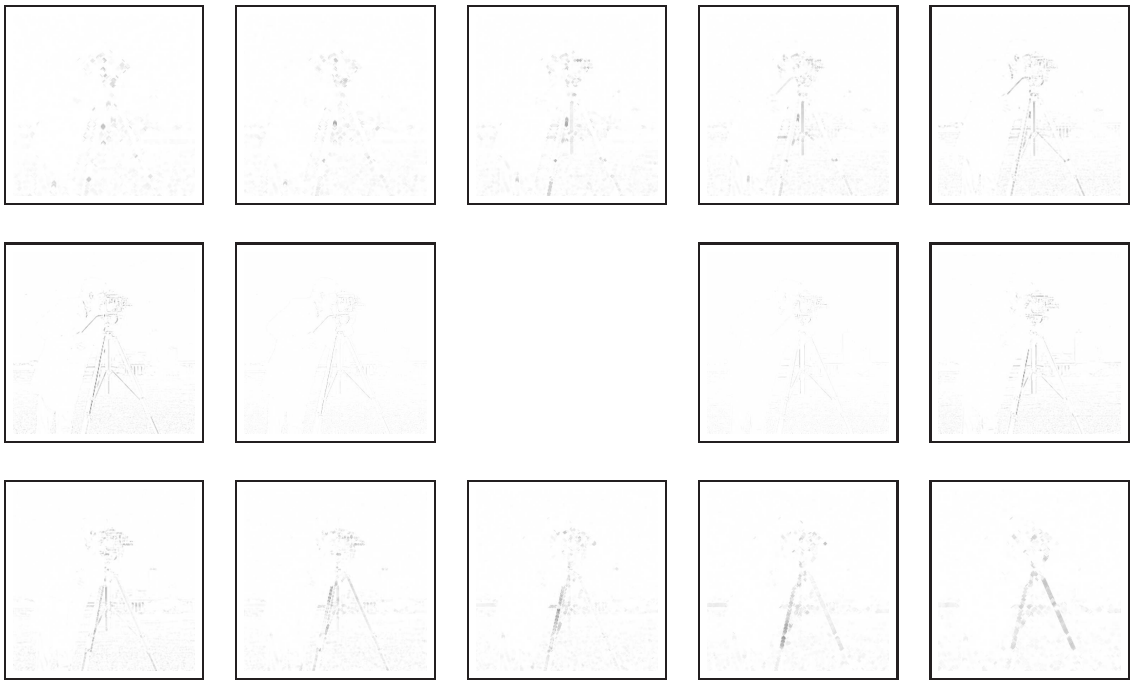

Figure 11: From top left to bottom right, Δ series of length $2n+1$ with $n=7$ using structural filters γ and φ and 4-connected elementary SE $\blacklozenge$. Grey levels have been inverted for the sake of readability.

on the desired properties of the series, one can even relax the constraint on the shape (compactness and convexity) of the SE in used.

Among these operators which do not belong to morphological filters, we can even use difference operators. For instance, by considering the morphological gradient $G_\lambda(f) = \delta_\lambda(f) - \varepsilon_\lambda(f)$ with increasing scale λ, we can build some morphological fractal measures [104]. Another example is related to top-hats and the so called hat scale-spaces [53]. More precisely, the top-hat by opening is defined by $\tau^\gamma(f) = f - \gamma(f)$ while the top-hat by closing (or bottom-hat) is defined by $\tau^\varphi(f) = \varphi(f) - f$. From these hat scale-spaces can be extracted the so called fingerprints introduced by Jackway and Deriche [52] as local maxima or minima in the images filtered at different scales λ. Fingerprints can also be obtained by the filters by reconstruction [89]. Various robust features can also be extracted from the analysis of scale-spaces made with top- and bottom-hat by reconstruction [64]. Of course we can also build other versions of these operators, e.g. using filters by reconstruction γ^ρ and φ^ρ. Any of the resulting series Π^{τ^ψ} can then be analysed in a similar manner as the standard Π series.

These different series are the basis of the standard morphological features widely used in image analysis and visual pattern recognition. These features are computed either at a local scale or a global scale.

2.2 Local morphological features

The simplest way to extract morphological features from a digital image f using one of the Π^ψ or Δ^ψ series consists in associating to each pixel p the vector $\Pi^\psi(f)(p) = (\Pi^\psi_\lambda(f)(p))_{0\leq\lambda\leq n}$ of size $n+1$.

In the remote sensing filed, this principle led to the so called differential morphological profile (DMP) proposed by Pesaresi and Benediktsson in [83, 21] which is computed using the reconstruction-based differential series:

$$\mathrm{DMP}(f)(p) = \Delta^\rho(f)(p) \tag{2.19}$$

Fig. 13 illustrates the behaviour of the DMP feature for pixels belonging to different areas of an image.

This feature is a kind of structural feature, and an interesting alternative to spectral or textural features. Its size (initially equal to $2n+1$) can be strongly reduced by considering only the few most

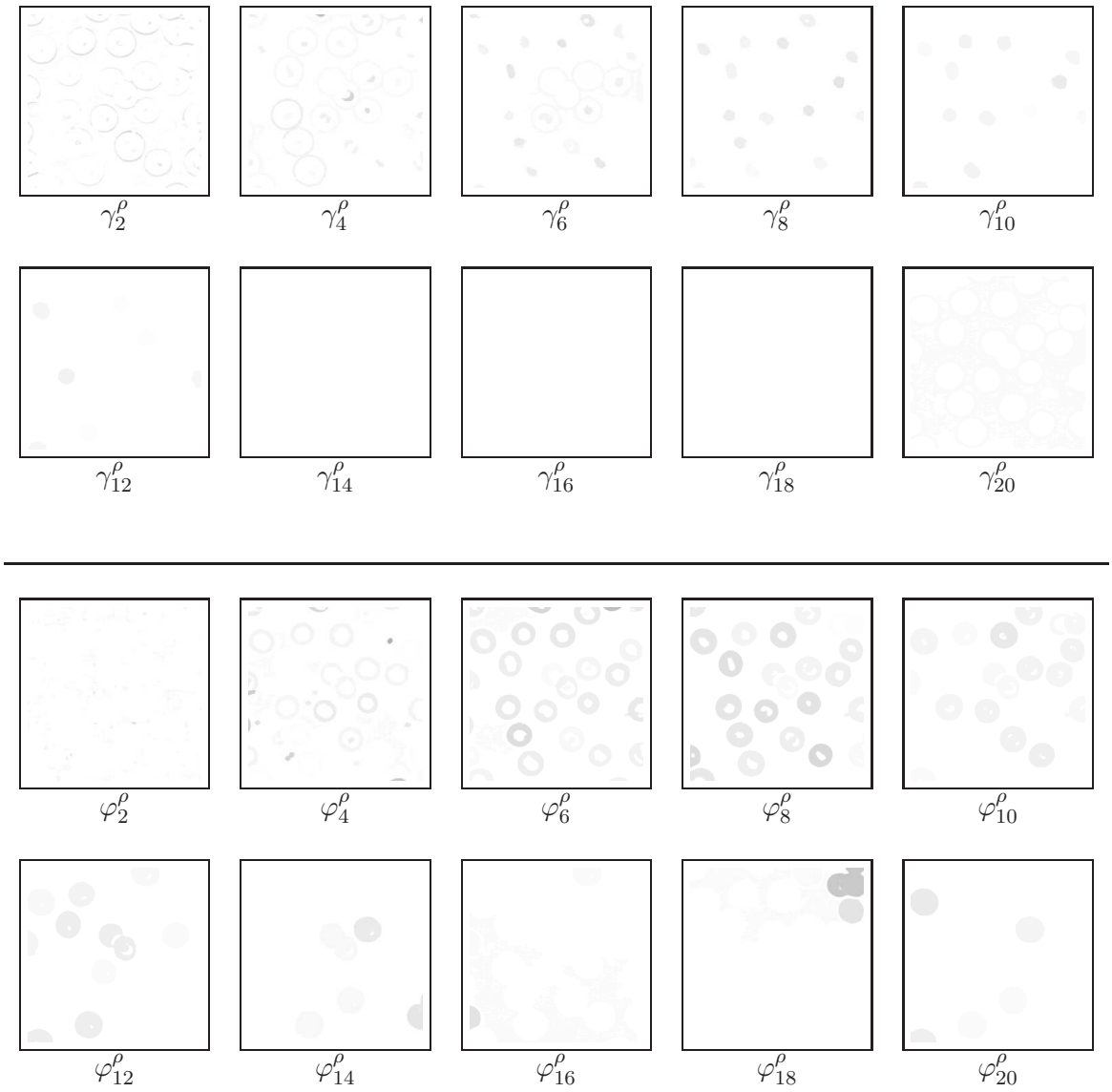

Figure 12: Details emphasised by means of differences between successive openings and closing by reconstruction. Grey levels have been inverted for the sake of readability.

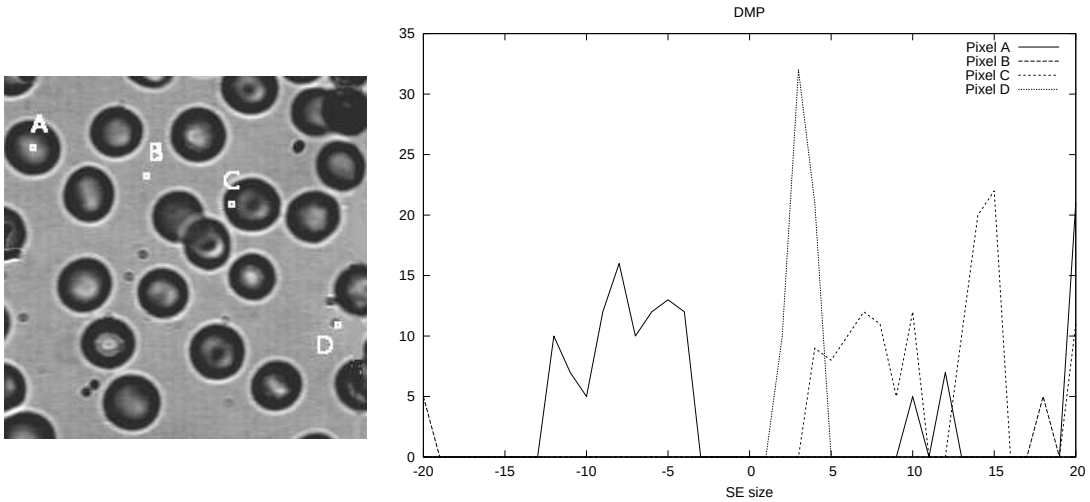

Figure 13: Input image with 4 sample points (left) and corresponding DMP values (right) using 20 openings (negative indices) and 20 closings (positive indices).

important maxima. It has been shown in [21] that using only the first and second maximum values of $\Delta^{\rho}(f)(p)$ for each pixel p ensures satisfactory recognition rates in supervised classification of remotely sensed images.

Moreover, an attempt has been made in [26] to use reconstruction-based alternate sequential filters through the $\Delta^{\mathrm{ASF}^{\rho}}$ series as an alternative to the original DMP, thus defining $\mathrm{DMP}_{\mathrm{ASF}}(f)(p) = \Delta^{\mathrm{ASF}^{\rho}}(f)(p)$. Alternatively, ASF-based scale-space representations can also be computed from the area-filters [2].

In case of binary images, pixelwise feature extraction from morphological scale-space may consist in assigning to each pixel p of f the scale, or size λ, for which the filter (e.g. opening) manages to remove the pixel, thus resulting in the so called opening transform when considering successive applications of the opening filter (similarly, the closing transform is related to the scale-space obtained from successive closings). The definition is given by:

$$\Xi^{\psi}(f)(p) = \max\{\lambda \geq 0 \mid \psi_{\lambda}(f)(p) > 0\} \tag{2.20}$$

with the convention $\Xi^{\psi}(f)(p) = 0$ if $f(p) = 0$. In other words, it can be easily computed by analysing the series Π and looking at each pixel p for the first image (with filter size $\lambda+1$) such as $\Pi^{\psi}_{\lambda+1}(f)(p) = 0$. Fig. 14 illustrates the opening and closing transforms considering various morphological filters and SE. The extension of this principle to greyscale images can lead to the definition of opening trees [122]. However, if one wants to keep a single value for each pixel, it is recommended to select the λ value resulting in the biggest drop in greyscale intensity when applying $\psi_{\lambda}(f)(p)$, thus following the recommendation of Pesaresi and Benediktsson with DMP.

2.3 Global morphological features

Besides the use of morphological series directly on a per-pixel basis, it is possible to involve them in global image features. In this case, pattern spectra and granulometries are certainly the most famous morphological features in the image analysis community [104].

Granulometries and antigranulometries (also called size and anti-size distributions) are built by gathering the values of the series over all pixels p of the filtered image $\psi(f)$ through a Lebesgue measure, for instance a volume or sum operation. In the particular case of binary images, the image volume can either be computed as the sum of pixel values or as the amount of white pixels (or 1-pixels).The granulometry uses openings:

$$\Omega^{\gamma}(f) = \left\{ \Omega^{\gamma}_{\lambda}(f) \mid \Omega^{\gamma}_{\lambda}(f) = \sum_{p \in E} \Pi^{\gamma}_{\lambda}(f)(p) \right\}_{0 \leq \lambda \leq n} \tag{2.21}$$

while the antigranulometry relies on closings:

$$\Omega^{\varphi}(f) = \left\{ \Omega^{\varphi}_{\lambda}(f) \mid \Omega^{\varphi}_{\lambda}(f) = \sum_{p \in E} \Pi^{\varphi}_{\lambda}(f)(p) \right\}_{0 \leq \lambda \leq n} \tag{2.22}$$

From the properties of morphological filters, we can observe that Ω^{γ} is monotonically decreasing while Ω^{φ} is monotonically increasing. In order these measures to be invariant to image size and to represent cumulative distribution functions, they are worth being normalised, thus resulting in the new definition:

$$\Gamma^{\psi}(f) = \left\{ \Gamma^{\psi}_{\lambda}(f) \mid \Gamma^{\psi}_{\lambda}(f) = 1 - \frac{\Omega^{\psi}_{\lambda}(f)}{\Omega^{\psi}_{0}(f)} \right\}_{0 \leq \lambda \leq n} \tag{2.23}$$

with ψ denoting either γ or φ. In Fig. 15 are given the granulometric curves Γ for both opening and closing filters, considering the main standard SE.

Another very interesting morphological global feature is the pattern spectrum Φ introduced by Maragos [68], also called pecstrum [3]. It can be seen as the morphological counterpart of the well-known

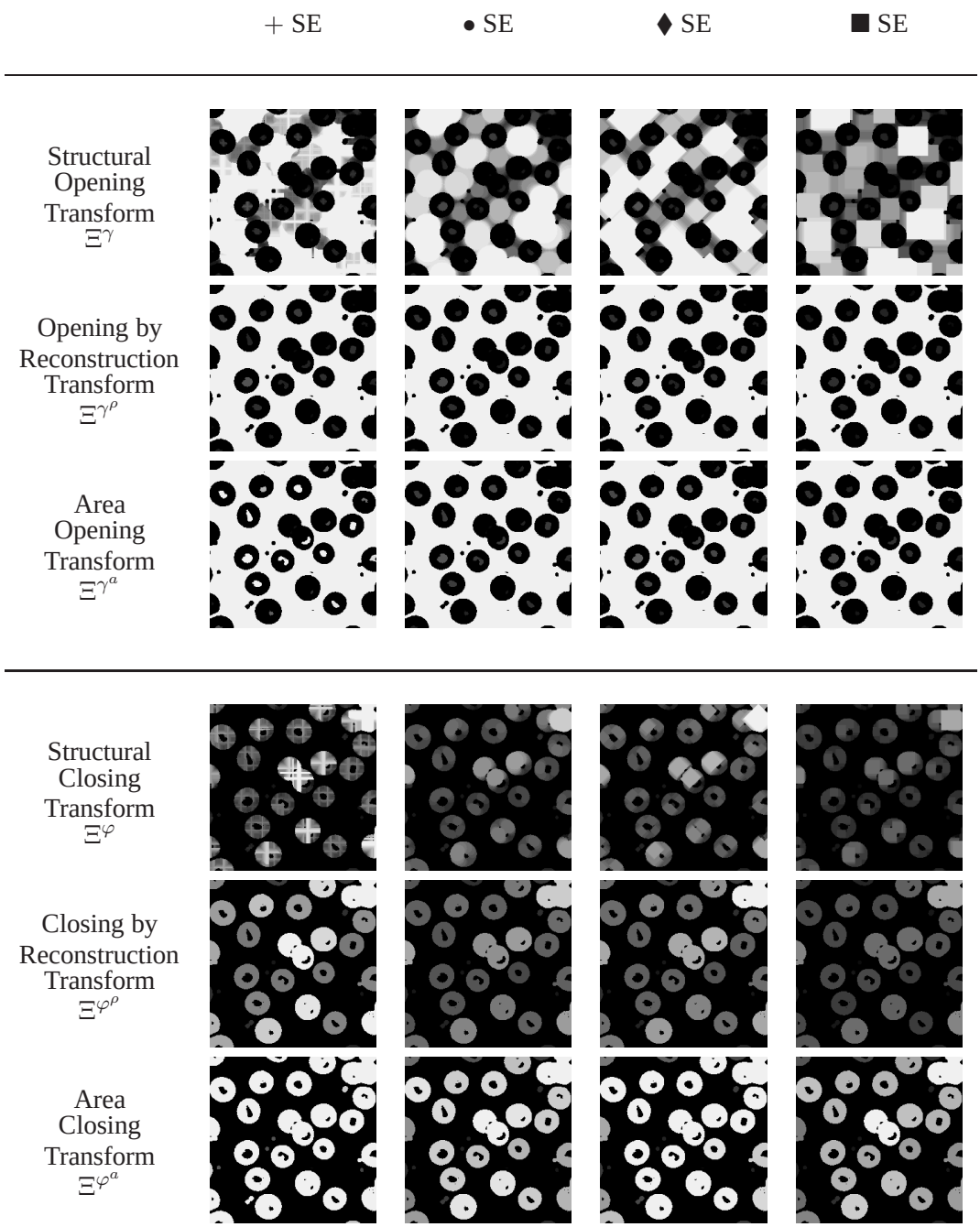

Figure 14: Illustration of various opening and closing transforms obtained with different filters and SE shapes.

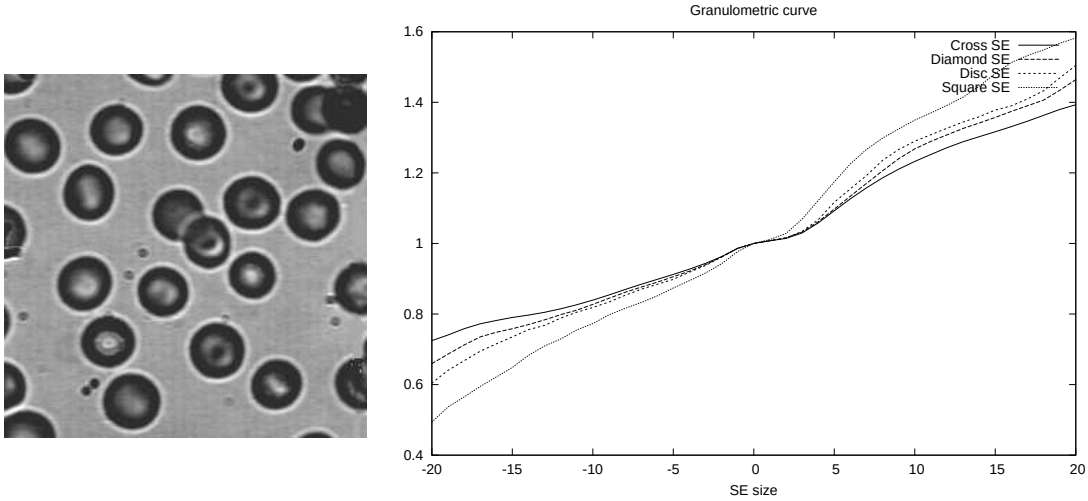

Figure 15: Input image (left) and corresponding granulometric curve Γ (right) using 20 openings (negative indices) and 20 closings (positive indices).

histogram. Instead of measuring the distribution of intensities within an image, it aims at measuring the distribution of sizes (and to a lesser extent, of shapes). To do so, it gathers values of the differential series Δ over all pixels:

$$\Phi(f) = \left\{ \Phi_\lambda(f) \mid \Phi_\lambda(f) = \sum_{p \in E} \Delta_\lambda(f)(p) \right\}_{-n \leq \lambda \leq n} \tag{2.24}$$

and the normalisation ensures measures independent of the image size:

$$\Lambda(f) = \left\{ \Lambda_\lambda(f) \mid \Lambda_\lambda(f) = \frac{\Phi_\lambda(f)}{\Omega_0(f)} \right\}_{-n \leq \lambda \leq n} \tag{2.25}$$

Moreover, let us notice that the pattern spectrum can be easily computed as the histogram of the opening (or/and closing) transform.

In Fig. 16 are given the pattern spectra Λ for both opening and closing filters, using respectively structural filters, filters by reconstruction and area filters. Moreover, Fig. 17 illustrates the relevance of the pattern spectrum in case of image with similar greylevel distribution.

When dealing with greyscale images, it is also possible to involve greyscale (or volume) SE, thus dealing with spatial but also to a lesser extent with intensity information.

Moreover, some scalar attributes can be extracted from the previous 1-D morphological series. As representative examples, we can cite the average size and roughness [68] computed respectively as the mean and the entropy of the signal, or the statistical moments computed on the granulometric 1-D curve and called granulometric moments [29, 98].

Besides the use of morphological filters to build global morphological filters, it is also possible to involve any operator ν and to exploit the morphological series (e.g. Π_ν) of images processed with this operator. In this case, the obtained series Ω_ν are called pseudo-granulometries since they do not respect the fundamental requirements of granulometries [104]. As another representative example of using Π_ν series, we can cite the covariance feature K, a morphological counterpart of the autocorrelation operator. To compute this feature, the SE b under consideration consists in a set of two points p_1 and p_2 and is defined by both a size $2\lambda = \|\overrightarrow{p_1 p_2}\|$ and an orientation $\vec{v} = \overrightarrow{p_1 p_2} / \|\overrightarrow{p_1 p_2}\|$:

$$K^{\vec{v}}(f) = \left\{ K^{\vec{v}}_\lambda(f) \mid K^{\vec{v}}_\lambda(f) = \sum_{p \in E} \Pi^{\varepsilon}_{\lambda, \vec{v}}(f)(p) \right\}_{0 \leq \lambda \leq n} \tag{2.26}$$

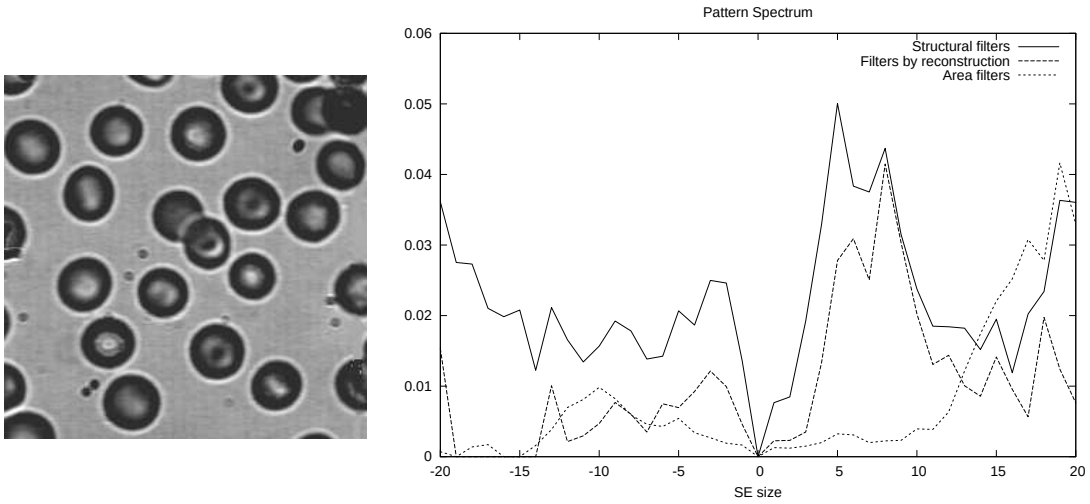

Figure 16: Input image (left) and corresponding pattern spectrum Λ (right) using structural filters, filters by reconstruction and area filters.

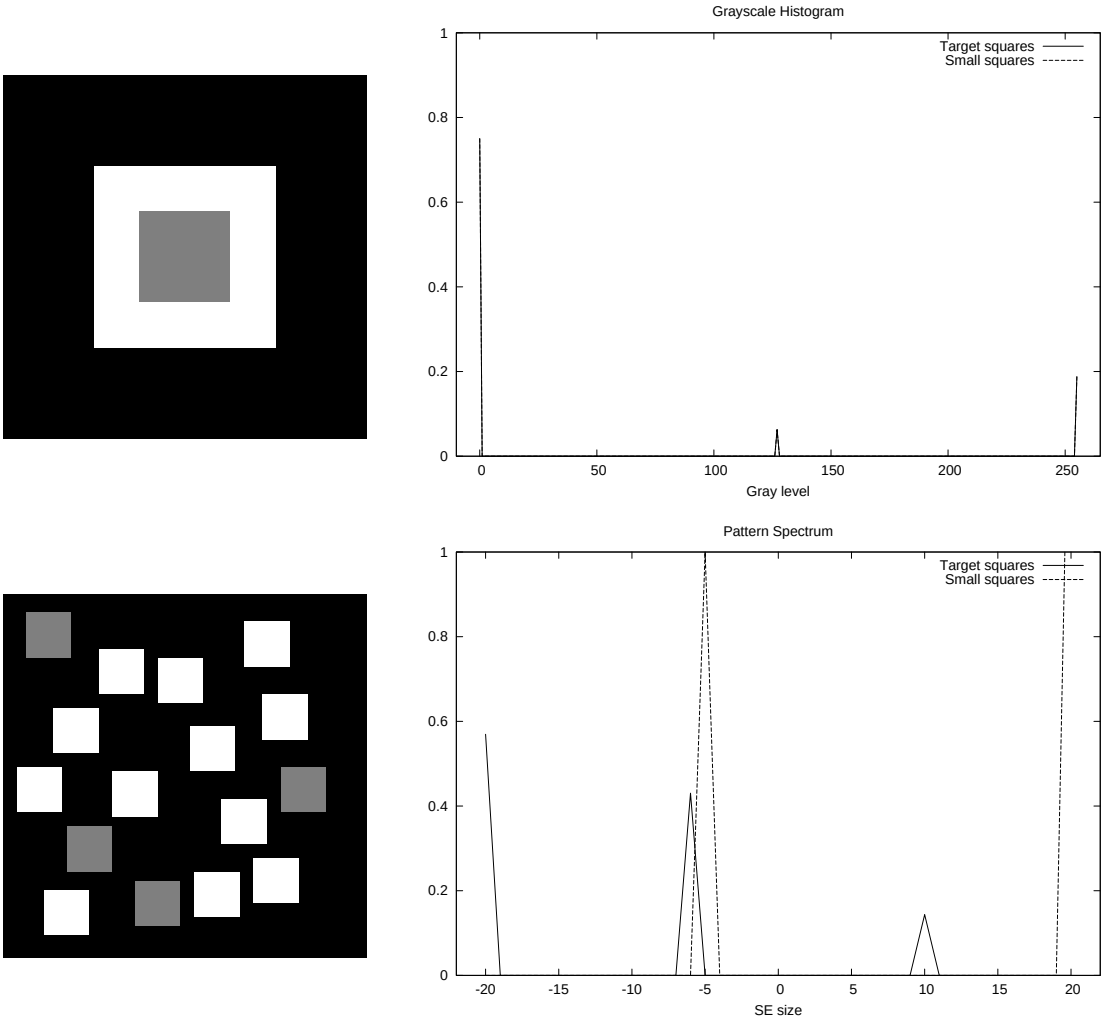

Figure 17: Two input image (left) with similar histograms (top right) but different pattern spectra Λ (bottom right).

where

$$\varepsilon_{\lambda,\vec{v}}(f)(p) = f(p - \lambda\vec{v}) \wedge f(p + \lambda\vec{v}) \tag{2.27}$$

This feature is illustrated by Fig. 18. Another definition of the covariance has been given by Serra [99] where the autocorrelation function is used, thus resulting in the operator ε' defined by

$$\varepsilon'_{\lambda,\vec{v}}(f)(p) = f(p - \lambda\vec{v}) \cdot f(p + \lambda\vec{v}) \tag{2.28}$$

where the intersection $\wedge$ is replaced by a product $\cdot$ operation.

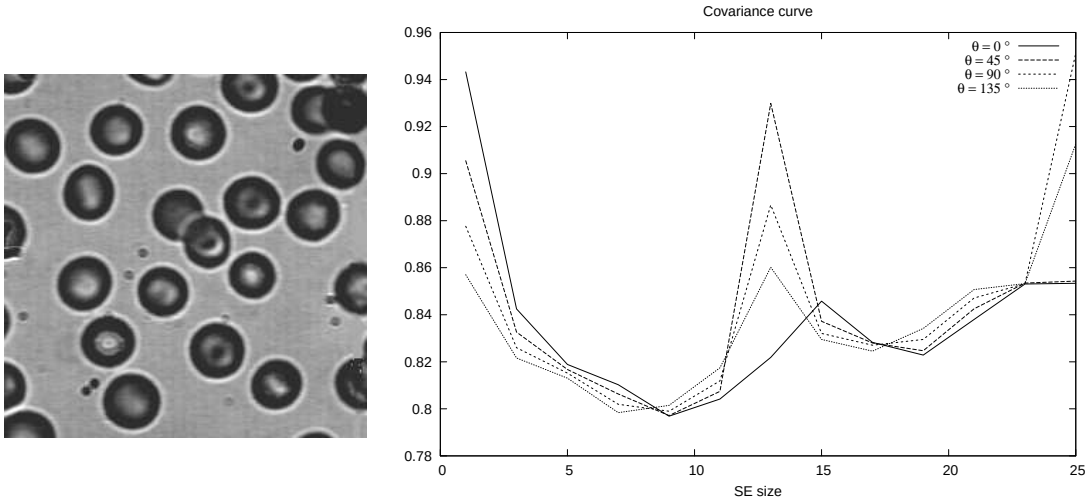

Figure 18: Input image (left) and corresponding covariance curves $K^{\vec{v}}$ (right) using 25 vector sizes λ and 4 different orientations θ for $\vec{v}$.

We have not dealt yet with the case of semi-local features, i.e. features computed on an intermediate scale. The processing units at this scale are neither the single pixels nor the whole image, but rather part of it, e.g. blocks or image regions. In this case, the global features can be computed similarly but within a limited area of the image, thus resulting in one morphological feature per block or region. An illustrative example of this approach is the work from Dougherty where each pixel is characterised by the granulometry computed from its neighbouring window [30].

Even if these features (either local or global) appear as particularly relevant alternatives to usual image features such as histograms, wavelets, or other textural features (just to mention a few), they still are limited to a single evolution curve and so cannot consider simultaneously several dimensions. More precisely, they deal only with the structural information extracted from morphological filters applied with growing SE sizes.

3 Multidimensional extensions of morphological features

Despite their broad interest in image representation, the well-known morphological features reviewed so far are limited by their one-dimensional nature (i.e. they are computed as single evolution curves and thus cannot consider simultaneously several dimensions).

We review here some recent multidimensional extensions which allow to build n-D (mostly 2-D) series of morphological measures. These extensions help to gather complementary information (e.g. spatial, intensity, spectral, shape, etc) in a single local or global morphological representation.

3.1 Size-shape

In the morphological series defined in the previous section, a unique parameter λ was considered for measuring the size evolution, through the SE b_λ. We have indicated various ways to build the series

of SE b_λ based on the increasing λ parameter. Here we consider the SE κ as a growing factor of the initial shape b, i.e. $b_\lambda = \delta_{\check{\kappa}}^{(\lambda-1)}(b)$ with various shapes for κ (e.g. one of the basic shapes introduced in section 1.2). Let us precise that the size of κ has to be rather small to build measurements at a precise scale (or conversely large for coarse measurements) since it represents the growing factor of the SE series. Moreover, one has also to set the initial condition b, i.e. the initial SE, which can be of arbitrary shape, even equal to κ (thus resulting in the definition given in section 1.2).

This definition assuming a single size varying parameter λ prevents us from performing accurate measurements. Indeed, it is not adequate to elliptical or rectangular shapes for instance, where the two independent axes should be taken into account. So several attempts have been made to build bivariate morphological series, thus allowing to obtain size-shape measurements.

Lefèvre et al. considers in [63] structuring elements with two different size parameters α and β that vary independently. More precisely, a way to define the 2-D series of SE $b_{\alpha,\beta}$ is given by $b_{\alpha,\beta} = \delta_{\check{\kappa}_1}^{(\alpha-1)}(\delta_{\check{\kappa}_2}^{(\beta-1)}(b)) = \delta_{\check{\kappa}_2}^{(\beta-1)}(\delta_{\check{\kappa}_1}^{(\alpha-1)}(b))$ with κ_1 and κ_2 denoting the structuring elements used as growing factors in the two dimensions, and b the initial SE. In the case of rectangular SE series, a relevant choice for κ_1 and κ_2 consists in 1-D SE such as horizontal and vertical lines respectively (with a length proportional to the degree of coarseness desired) and an initial rectangular SE b.

The new Π series built using the 2-D set of SE $b_{\alpha,\beta}$ is then computed as:

$$\Pi^\psi(f) = \left\{ \Pi^\psi_{\alpha,\beta}(f) \mid \Pi^\psi_{\alpha,\beta}(f) = \psi_{\alpha,\beta}(f) \right\}_{\substack{0\le\alpha\le m \\ 0\le\beta\le n}} \tag{3.1}$$

where the application of ψ on f with a SE $b_{\alpha,\beta}$ is noted $\psi_{\alpha,\beta}(f)$ and with the convention $\psi_{0,0}(f) = f$. Similarly, the Δ series measures the differential in both size dimensions:

$$\Delta^\psi(f) = \left\{ \Delta^\psi_{\alpha,\beta}(f) \mid \Delta^\psi_{\alpha,\beta}(f) = \frac{1}{2} \left| 2\Pi^\psi_{\alpha-1,\beta-1}(f) - \Pi^\psi_{\alpha-1,\beta} - \Pi^\psi_{\alpha,\beta-1}(f) \right| \right\}_{\substack{0\le\alpha\le m \\ 0\le\beta\le n}} \tag{3.2}$$

where $\Delta^\psi_{\alpha,0} = \Delta^\psi_\alpha$, $\Delta^\psi_{0,\beta} = \Delta^\psi_\beta$, and $\Delta^\psi_{0,0} = 0$.

Fig. 19 illustrates the potential interest of such 2-D features for sample images where standard granulometries are irrelevant.

A similar approach has been proposed by Ghosh and Chanda [40] who introduce conditional parametric morphological operators, and who build a 2D set of SE with increasing size, both on the horizontal and vertical dimensions. From this set of SE they finally compute the bivariate pattern spectrum for binary images. Bagdanov and Worring introduce the same feature under the term rectangular granulometry [13], while a slightly different definition has been given by Barnich et al [17] to limit the SE to the largest non-redundant rectangles within the analysed object (in binary images). Moreover, a more general expression of m-parametric SE has been used in [37] to define multiparametric granulometries.

Batman et al. in [18, 19] propose an alternative definition of this series using Euclidean series $\Pi^{\psi^\alpha}(f)$ with the set of SE $B = \{-_1, |_1\}$ where $-$ and $|$ denote respectively elementary horizontal and vertical SE. Moreover, they also introduce a univariate series by combining through the sum operations two series of SE b_α and c_β built from initial SE b and c:

$$\Pi^\psi(f) = \left\{ \Pi^\psi_{\alpha,\beta}(f) \mid \Pi^\psi_{\alpha,\beta}(f) = \psi_{b_\alpha}(f) + \psi_{c_\beta}(f) \right\}_{\substack{0\le\alpha\le m \\ 0\le\beta\le n}} \tag{3.3}$$

Urban and Wilkinson [114] also propose to combine size and shape information in a single 2-D granulometry. They rely on attribute filters [25] ψ^χ and use a max-tree representation [97] of the image for computational reasons. Their 2-D series can be defined as:

$$\Pi^{\psi^{\chi_1,\chi_2}}(f) = \left\{ \Pi^\psi_{\alpha,\beta}(f) \mid \Pi^\psi_{\alpha,\beta}(f) = \psi^{\chi_1}_\alpha(f) \wedge \psi^{\chi_2}_\beta(f) \right\}_{\substack{0\le\alpha\le m \\ 0\le\beta\le n}} \tag{3.4}$$

where the two criteria χ_1 and χ_2 are respectively related to the area (i.e. defining size) and the ratio of the moment of inertia to the square of the area (i.e. defining shape). While the first dimension (indexed

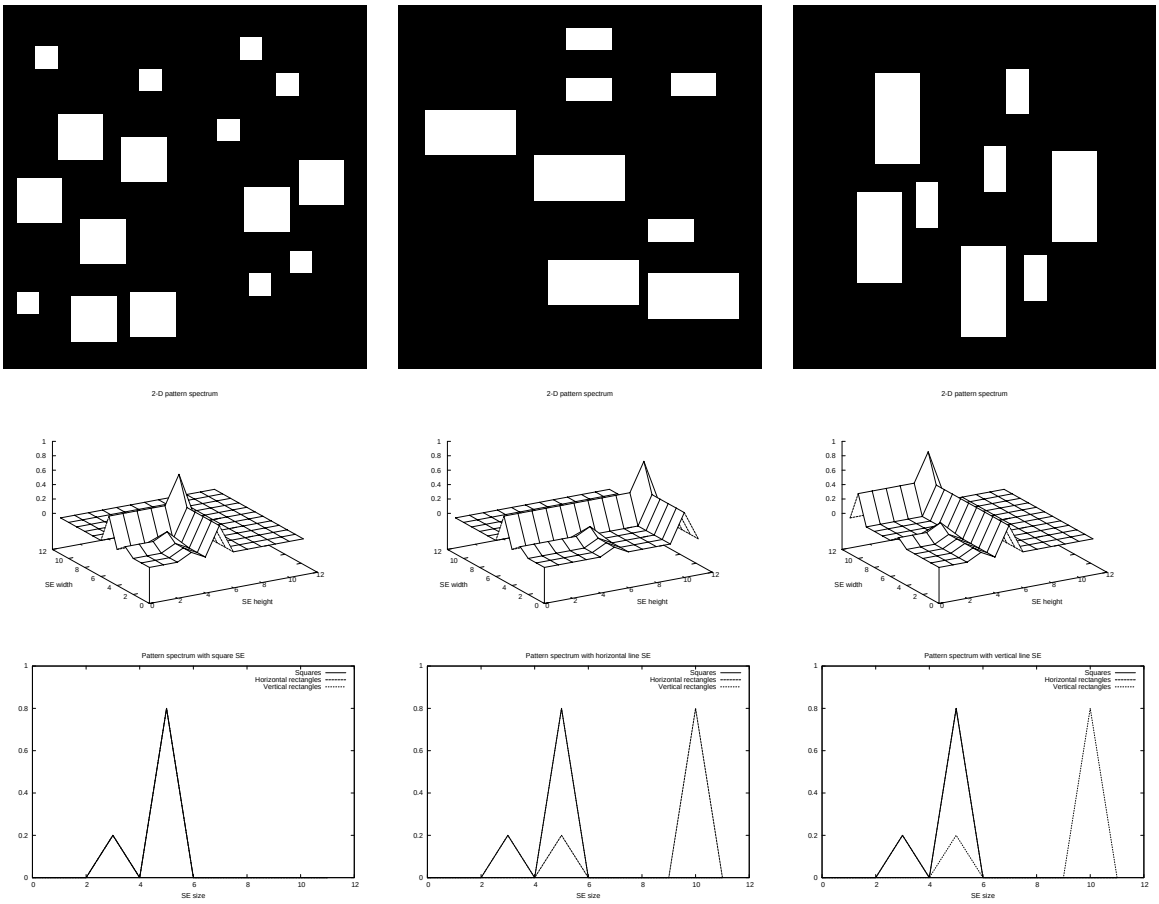

Figure 19: Three input images (top) and their respective 2-D Δ feature (middle). As a comparison, standard pattern spectra using square SE (bottom left), horizontal line SE (bottom centre) and vertical line SE (bottom right) are also given.

by α and related to the criterion χ_1) is related to size and respect the axioms of morphological scale-spaces, the second dimension (indexed by β and related to the criterion χ_2) is related to shape and should be scale-invariant, thus the increasingness property is replaced by the scale-invariance property, i.e. $S_\lambda(\Upsilon_t(f)) = \Upsilon_t(S_\lambda(f)),\ \forall t > 0$ with the transform $S_\lambda(f)$ being the scaling of the image f by a scalar factor λ.

3.2 Size-orientation

Besides the size of the SE, one can also vary its orientation [126]. Naturally this is relevant only with anistropic structuring elements and not for disc-shaped SE, nor with area-based filters. Let us note $b_{\lambda,\theta}$ a SE of size λ and orientation θ. This SE is built from a rotation of the initial SE b_λ with an angle θ, i.e. $\measuredangle(b_\lambda, b_{\lambda,\theta}) = \theta$ with $\measuredangle(b_1, b_2)$ the measured angle between orientations of b_1 and b_2.

Based on this principle, the morphological series is then defined as:

$$\Pi^\psi(f) = \left\{ \Pi^\psi_{\lambda,\theta}(f) \mid \Pi^\psi_{\lambda,\theta}(f) = \psi_{\lambda,\theta}(f) \right\}_{\substack{0 \le \lambda \le n \\ \theta_0 \le \theta \le \theta_m}} \tag{3.5}$$

where $\{\theta_0, \ldots, \theta_m\}$ represents the set (of cardinality $|\theta|$) of orientations considered, and $\psi_{\lambda,\theta}$ is a shortcut for $\psi_{b_{\lambda,\theta}}$. Fig. 20 illustrates the interest of such size-orientation features when the standard granulometry is useless.

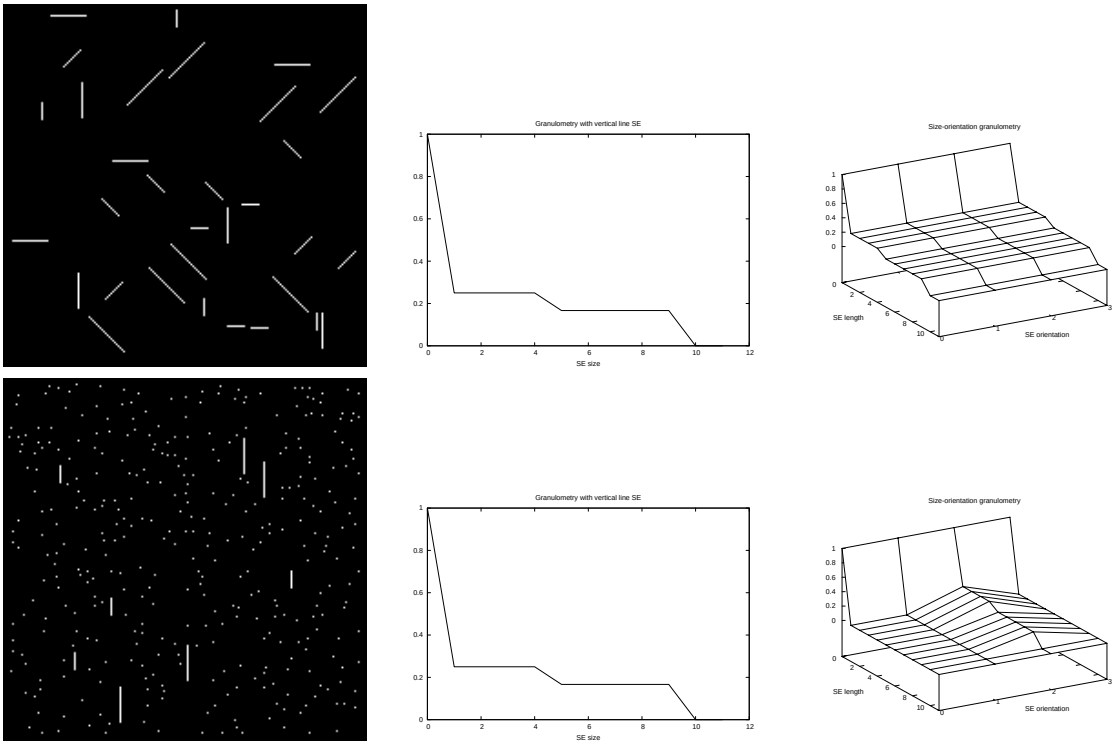

Figure 20: Two input images (left), their respective (similar) granulometric curve with vertical SE (centre) and their 2-D size-orientation granulometric curve (right) considering four angles.

Apart from the most simple angles (i.e. $\theta = k\pi/4$), one has to tackle very carefully the problem of discretisation for rotated SE. Accurate approximations can be obtained by periodic lines (see the work from Jones and Soille [58]) and require the use of several SE to get an accurate discrete representation of a continuous segment [105]. It is also possible to retain for each pixel at a given size, only the maximum or minimum value from the results returned by the morphological filter with the various orientations [68]. In this case however, the result is a 1-D series similar to the one which could be obtained by means of radial filters [104]. Finally, from these size-orientation measures, other features can be extracted such as orientation maps proposed by Soille and Talbot [105].

3.3 Size-spectral or size-colour

Since digital images contain very often spectral or colour information, it is worth involving the spectral signature or colour of each pixel in the computation of the morphological representation.

To do so, it is possible to first compute a morphological signature for each of the k spectral components (or bands) and then to combine these k signatures into a single one. With this two-step approach, the morphological series Π can be expressed as:

$$\Pi^{\psi}(\mathbf{f}) = \left\{ \Pi^{\psi}_{\lambda,\omega}(\mathbf{f}) \mid \Pi^{\psi}_{\lambda,\omega}(\mathbf{f}) = \psi_{\lambda}(f_{\omega}) \right\}_{\substack{1 \leq \omega \leq k \\ 0 \leq \lambda \leq n}} \tag{3.6}$$

where f_{ω} is a greyscale image representing the ω^{th} spectral component of the multispectral or colour image $\mathbf{f} = \{f_w\}_{1 \leq \omega \leq k}$. In this definition, morphological filters are applied independently on each image band, thus the marginal strategy is used and the correlation among the different spectral channels is completely ignored. Moreover it can result in new spectral signatures or colours in the filtered images.

To avoid these limitations, it is possible to rather consider a vectorial ordering when applying the morphological operators on the multispectral input image $\mathbf{f}$ [5]. The purpose of a vectorial ordering is to give a way to order vectors and thus to compute vectorial extrema by means of the two operators $\sup^{v}$ and $\inf^{v}$. Assuming a given vectorial ordering, the fundamental dilation and erosion operators are written:

$$\varepsilon^{v}_{b}(\mathbf{f})(p) = \inf^{v}_{q \in b} \mathbf{f}(p+q), \quad p \in E \tag{3.7}$$

$$\delta^{v}_{b}(\mathbf{f})(p) = \sup^{v}_{q \in b} \mathbf{f}(p-q), \quad p \in E \tag{3.8}$$

and from these operators it is possible to write all vectorial versions of the morphological operators described previously in this chapter.

The new size-spectral morphological series is finally computed as:

$$\Pi^{\psi}(\mathbf{f}) = \left\{ \Pi^{\psi}_{\lambda,\omega}(\mathbf{f}) \mid \Pi^{\psi}_{\lambda,\omega}(\mathbf{f}) = \left(\psi^{v}_{\lambda}(\mathbf{f})\right)_{\omega} \right\}_{\substack{1 \leq \omega \leq k \\ 0 \leq \lambda \leq n}} \tag{3.9}$$

where $\left(\psi^{v}_{\lambda}(\mathbf{f})\right)_{\omega} = \psi_{\lambda}(f_{\omega})$ in the specific case of a marginal ordering. A comparison of marginal and vectorial strategies is given in Fig. 21, considering a similar size distribution but a different spatial distribution in each colour band.

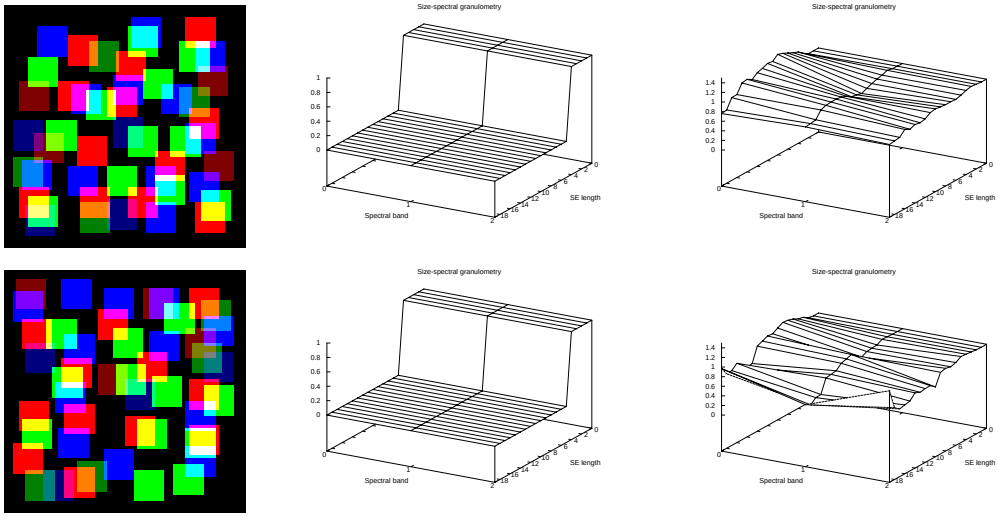

Figure 21: Two input images (left), their respective granulometric curves computed with a marginal strategy (centre) and with a vectorial strategy (right).

For a comprehensive review of vectorial orderings and multivariate mathematical morphology, the reader can refer to the survey from Aptoula and Lefèvre [5]. An example of colour pattern spectrum can be found in [61] while a comparison between several vectorial orderings has also been proposed recently by Gimenez and Evans [42] using the series $\Pi^{\mathrm{ASF}^{\alpha}}(\mathbf{f})$. In [79], Nes and d'Ornellas consider colour pattern spectra with linear SE of variable directions (at each scale λ, the maximum pattern spectrum among the various orientations is selected). In [90], Rivest deals with radar signals and propose adequate granulometry and power spectrum by introducing a vector ordering dedicated to complex data.

3.4 Size-intensity

In greyscale images, the pixel intensity values are used either directly (at local scale) or gathered with the sum operator (at global scale). So the distribution of intensity values in the image is not taken into account with standard morphological features, which can be a real issue since intensity distribution (usually measured by an histogram) is a key feature to represent image content.

Computing the histogram on morphological scale-spaces has been proposed by Lefèvre in [62] to take into account both size and intensity distributions. To do so, let us use the Kronecker delta function:

$$\delta_{i,j} = \begin{cases} 1 & \text{if } i = j \\ 0 & \text{if } i \neq j \end{cases} \tag{3.10}$$

and the histogram function $h_f : T \to \mathbb{Z}$:

$$h_f(\eta) = \sum_{p \in E} \delta_{\eta, f(p)} \tag{3.11}$$

which measures the number of occurrences of each greylevel η in the image f. Alternatively, we can also use the normalised histogram function $h'_f : T \to [0,1]$ where

$$h'_f(\eta) = \frac{h_f(\eta)}{|\operatorname{supp}(f)|} \tag{3.12}$$

with $|\operatorname{supp}(f)|$ the cardinality of the support of f, i.e. the number of pixels in f.

The formulation of the 2-D size-intensity morphological feature is then given by the following Π series:

$$\Pi^{\psi}(f) = \left\{ \Pi^{\psi}_{\lambda,\eta}(f) \mid \Pi^{\psi}_{\lambda,\eta}(f) = h_{\psi_\lambda(f)}(\eta) \right\}_{\substack{\eta_0 \leq \eta \leq \eta_m \\ 0 \leq \lambda \leq n}} \tag{3.13}$$

where $\{\eta_0, \ldots, \eta_m\}$ represents the different greylevels or bins in the histogram.

Fig. 22 shows the relevance of size-intensity morphological features when both granulometry and histogram are irrelevant. For the sake of clarity, greylevel 0 (i.e. black pixels) as been omitted in the plots.

Its derivative counterpart can be given by the following Δ series:

$$\Delta^{\psi}(f) = \left\{ \Delta^{\psi}_{\lambda,\eta}(f) \mid \Delta^{\psi}_{\lambda,\eta}(f) = h_{\psi_\lambda(f) - \psi_{\lambda-1}(f)}(\eta) \right\}_{\substack{\eta_0 \leq \eta \leq \eta_m \\ 0 \leq \lambda \leq n}} \tag{3.14}$$

This feature can be seen as a morphological alternative to the very effective multiresolution histograms computed from Gaussian linear scale-spaces [44].

Spatial and intensity information can also be gathered by the use of structuring functions (SF) as proposed by Lotufo and Trettel [66]. More precisely, let us define the SF $g_{\lambda,\eta}$ as a non-planar cylinder of radius λ and amplitude η. A size-intensity feature is then built using various λ and η values:

$$\Pi^{\psi}(f) = \left\{ \Pi^{\psi}_{\lambda,\eta}(f) \mid \Pi^{\psi}_{\lambda,\eta}(f) = \psi_{\lambda,\eta}(f) \right\}_{\substack{\eta_0 \leq \eta \leq \eta_m \\ 0 \leq \lambda \leq n}} \tag{3.15}$$

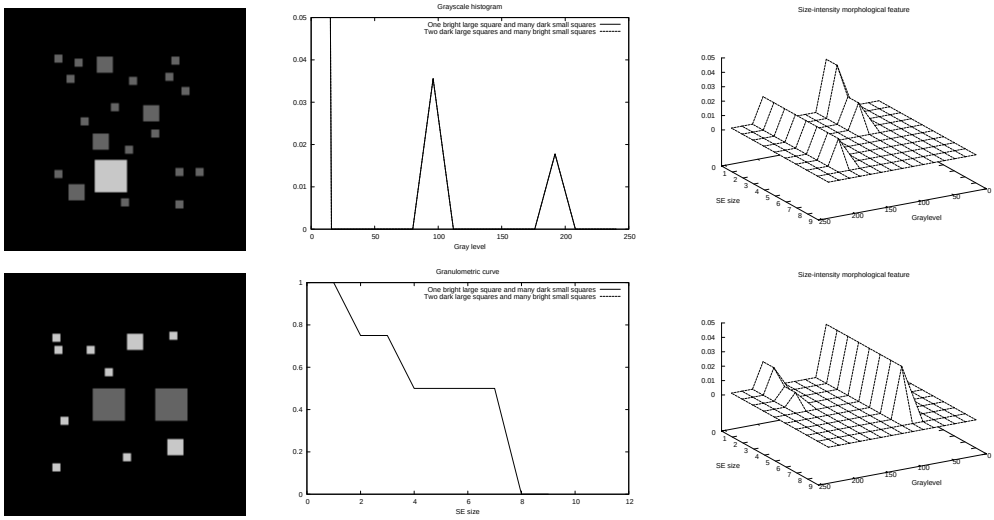

Figure 22: Two input images (left) with similar histogram (top centre) and granulometry (bottom centre), but with different size-intensity morphological features (right).

where $\psi_{\lambda,\eta}$ is here a shortcut for $\psi_{g_{\lambda,\eta}}$. It has been noticed in [66] that both the classic histogram and the pattern spectrum can be derived from this measure by considering respectively $\lambda = 0$ (i.e. a single pixel) and $\eta = 0$ (i.e. a flat disc-shaped SE).

A similar feature called granold has been proposed by Jones and Jackway [57] by first decomposing the greyscale image into a stack of binary images and then computing the granulometry for each binary image (i.e. at each greyscale threshold), thus resulting in the following series:

$$\Pi^{\psi}(f) = \left\{ \Pi^{\psi}_{\lambda,\eta}(f) \mid \Pi^{\psi}_{\lambda,\eta}(f) = \psi_{\lambda}(T_{\eta}(f)) \right\}_{\substack{\eta_0 \leq \eta \leq \eta_m \\ 0 \leq \lambda \leq n}} \tag{3.16}$$

where T_{η} denotes the thresholding function:

$$T_{\eta}(f)(p) = \begin{cases} 1 & \text{if } f(p) \geq \eta \\ 0 & \text{if } f(p) < \eta \end{cases} \tag{3.17}$$

Despite their different definitions, both [66] and [57] lead to similar measures.

3.5 Size-spatial

All the previous features were considering the spatial information through the successive applications of morphological operators which rely on a spatial neighbourhood. But they did not retain any information about the spatial distribution of the pixels at a given scale λ. A first attempt to deal with this problem was made by Wilkinson [127] who proposed to compute spatial moments on the filtered binary images, thus resulting in spatial pattern spectra:

$$\Phi(f) = \{ \Phi_{\lambda}(f) \mid \Phi_{\lambda}(f) = m_{ij}\left(\Delta_{\lambda}(f)\right) \}_{\substack{m_{ij} \\ -n \leq \lambda \leq n}} \tag{3.18}$$

where m_{ij} denotes the moment of order (i, j), computed on an image f as:

$$m_{ij}(f) = \sum_{(x,y) \in E} x^i y^j f(x, y) \tag{3.19}$$

This idea was later followed by Aptoula and Lefèvre in [4] where a normalised spatial covariance involving normalised unscaled central moments μ_{ij} is proposed to ensure scale and translation invariance:

$$K^{\vec{v}}(f) = \left\{ K^{\vec{v}}_{\lambda} \mid K^{\vec{v}}_{\lambda} = \mu_{ij}\left(\Pi^{\varepsilon}_{\lambda,\vec{v}}(f)(p)\right) / \mu_{ij}(f) \right\}_{\substack{\mu_{ij} \\ 0 \leq \lambda \leq n}} \tag{3.20}$$

with μ_{ij} defined by:

$$\mu_{ij}(f) = \frac{\sum\limits_{(x,y)\in E} (x-\bar{x})^i (y-\bar{y})^j f(x,y)}{(m_{00}(f))^\alpha} \text{ with } \alpha = \frac{i+j}{2}+1, \ \ \forall i+j \geq 2 \tag{3.21}$$

and $\bar{x} = m_{10}(f)/m_{00}(f)$, $\bar{y} = m_{01}(f)/m_{00}(f)$.

Alternatively, Ayala and Domingo proposed spatial size distributions [11] where filtered images of the morphological series are replaced by their intersection with filtered translated images, intersection being computed on a linear way with a product rather than on a nonlinear way with a minimum. Thus their feature can be obtained by comparing the linear covariances applied on both initial and filtered images, for all possible vectors in a set defined by κb, with increasing κ values:

$$\Omega(f) = \left\{ \Omega_{\lambda,\kappa} \mid \Omega_{\lambda,\kappa} = \frac{1}{\left(\sum\limits_{p\in E} f(p)\right)^2} \sum_{q\in\kappa b} K_1'^{\vec{q}}(f) - K_1'^{\vec{q}}(\Pi_\lambda(f)) \right\}_{\substack{0\leq\kappa\leq k \\ 0\leq\lambda\leq n}} \tag{3.22}$$

where $\vec{q}$ is a shortcut for the vector $\overrightarrow{oq}$ with o the centre or origin of the SE b, and q any neighbour belonging to the SE. Here we have used the notation K' to denote the autocorrelation function (cf. section 2.3). The spatial-size distribution can finally be computed as a 2-D differential measure, in a way similar to the computation of the Δ measure from the associated Π one. Zingman et al. [138] propose the pattern density spectrum with a rather similar definition but relying on some concepts of fuzzy sets (actually their density opening operator is similar to a rank-max opening [104]). Combined with the standard pattern spectrum, they obtain the 2D size-density spectrum.

Finally, Aptoula and Lefèvre [6] consider a composite SE built from two different SE, and introduce two parameters λ and κ to deal with both the size of the two SE and the shift between them. Their new operator combines the filtering properties of the granulometry and the covariance, thus resulting in a series:

$$\Pi^{\psi,\vec{v}}(f) = \left\{ \Pi^{\psi,\vec{v}}_{\lambda,\kappa}(f) \mid \Pi^{\psi,\vec{v}}_{\lambda,\kappa}(f) = \psi_{\lambda,\kappa\vec{v}}(f) \right\}_{\substack{0\leq\kappa k \\ 0\leq\lambda\leq n}} \tag{3.23}$$

with $\psi_{\lambda,\kappa\vec{v}}$ a shortcut for $\psi_{b_{\lambda,\kappa\vec{v}}}$, and the composite SE being defined as $b_{\lambda,\kappa\vec{v}} = b_\lambda \cup (b_\lambda + \kappa\vec{v})$, i.e. a pair of SE b of size λ separated by a vector $\kappa\vec{v}$. The following normalised measure can then be computed from the previous series:

$$\Gamma^{\psi,\vec{v}}(f) = \left\{ \Gamma^{\psi,\vec{v}}_{\lambda,\kappa}(f) \mid \Gamma^{\psi,\vec{v}}_{\lambda,\kappa}(f) = \frac{\sum_{p\in E} \Pi^{\psi,\vec{v}}_{\lambda,\kappa}(f)(p)}{\sum_{p\in E} f(p)} \right\}_{\substack{0\leq\kappa k \\ 0\leq\lambda\leq n}} \tag{3.24}$$

Fig. 23 illustrates the interest of size-spatial features, considering the spatial covariance defined in Eq. (3.20) with vertical information taken into account.

We have presented various features which can be extracted from morphological scale-spaces. We will now discuss the issues related to their practical implementation.

4 Practical implementation issues

In support with the theoretical presentation introduced above, we discuss here the issues related to the practical implementation of morphological features. Naturally, straight coding of the features described previously will lead to prohibitive computation time, thus making morphological features irrelevant for most of the real-life problems. However a lot of work has been done on efficient algorithms and operators in the field of mathematical morphology. So all the features presented in the previous sections can be computed very efficiently and thus be involved actually in any real (even real-time) system. Moreover, other issues have often to be taken into account, for instance noise robustness, definition of optimal parameters, etc.

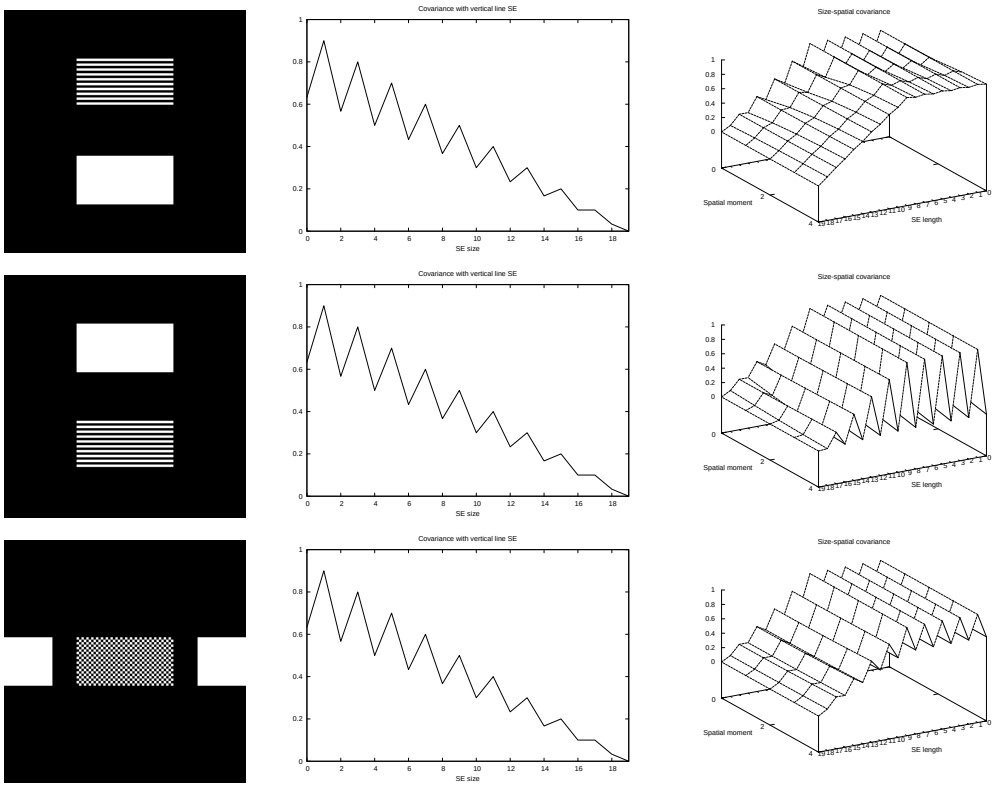

Figure 23: Three input images (left), their respective covariance curve with vertical SE (centre) and 2-D size-spatial granulometric curve (right) considering vertical spatial moments.

4.1 Efficient algorithms

Features presented previously need the application of a given morphological filter many times to build the scale-space from which they can be extracted.

In case of features based on standard filters (e.g. structural openings and closings), the reader will find in the paper of Luc Vincent [122] a comprehensive set of fast algorithms. We recall here the main ideas of this paper. When dealing with binary images, two different cases have to be considered. The most simple case is related to linear SE for which a run-length technique can be involved. The principle for horizontal SE is to scan each line of the image from left to right, and add the length λ of each discovered run (i.e. series of successive white pixels) to the associated Φ_λ bin of the pattern spectrum Φ. With more complex SE, creating an opening transform is most of the time a prerequisite for fast algorithms, and can be performed using a distance transform. Once the opening transform has been computed, extracting the granulometry or pattern spectrum is very straightforward. In [122] are given very efficient algorithms compatible with SE which can be decomposed into most simple ones (horizontal, vertical or diagonal SE). The distance transform computed with city-block distance metric may also be an appropriate basis for disc-shaped SE [41]. In his paper, Vincent has extended the opening transform for binary images to the opening tree for greyscale images. Linear SE are tackled with a run-length technique rather similar to the binary case, with an additional step which consists in opening the segments found in the input image iteratively to fill all the related bins in the pattern spectrum. For the other kinds of SE (from which a decomposition into simple SE is possible), it is necessary to compute an opening tree. In such a structure, each node represents a plateau in the image (i.e. a series of successive pixels having a value higher or equal to a level l). The tree root is related to the lowest level $l = 0$ while the leaves correspond to local maxima. The pattern spectrum can then be obtained by analysing the successive nodes of the opening tree for each pixel. Vincent also introduces some techniques to deal with semi-local computation of granulometries.

As far as attribute-based operators are concerned, several efficient algorithms have also been pro-

posed. Vincent introduces in [121] an algorithm for area-based filters which starts from all image maxima and iteratively analyse their neighbourhoods by increasing the greyscale range until the area parameter is reached. His work was extended to general attribute-based filters by Breen and Jones [25], while Salembier et al. [97] introduced another solution for attribute-based filters using new data structures, the max and min tree. More recently, Meijster and Wilkinson [74] give an alternative solution to the use of queues based on the very efficient union-find structure and compare their approach with previously cited works.

In order to reduce the computation time, it is necessary to limit the number of comparisons needed when applying a morphological operator. This can be achieved either by decomposing a 2-D SE into smaller (either 1-D or 2-D SE), or by optimising a given morphological operator through analysis of its behaviour (in particular with linear SE), and a recent review has been made by van Droogenbroeck and Buckley [118] (the case of filters using a rectangular SE is considered in a previous paper from van Droogenbroeck [117]). To illustrate the first case, let us assume a SE b can be written as a combination of smaller SE b_1 and b_2 such as $b = \delta_{\check{b_1}} b_2$. Then the morphological filtering simplifies: $\phi_b(f) = \phi_{b_1}\phi_{b_2}(f)$. Similarly, the SE b with size λ can be defined as $b_\lambda = \lambda b = \delta_{\check{b}}^{(\lambda-1)}(b)$. Thus various solutions have been introduced in the literature for SE decomposition, mainly dealing with convex flat SE. Among the earliest works, Zhuang and Haralick proposed an efficient tree search technique [131] and later on Park and Chin [81] consider the decomposition of a SE into its prime factors. More recently, Hashimoto and Barrera introduced a greedy algorithm which minimises the number of SE used in the decomposition [46]. But all the deterministic approaches are related to convex SE, some are even dedicated to a particular shape (e.g. a disc in [119]). When dealing with nonconvex SE, solutions can be obtained through the use of genetic algorithms [101] or linear programming [132] for instance. In case of structuring functions, one can refer for instance to the work of Engbers et al [33]. Moreover, it is also possible to perform a 1.5-D scan of the 2-D SE as proposed by Fredembach and Finlayson [36]. To the best knowledge of the author, the most up-to-date technique is from Urban and Wilkinson [115] who do not decompose a SE into smaller SE but into chords, and for which the C source code is freely available from the authors.

Besides efficient algorithms to ensure low computation time, one can also rely on hardware implementation of the morphological operators [75, 102]. In case of hyperspectral data, Plaza et al. consider a parallel architecture built from a cluster of workstations [86].

4.2 Robustness and adaptation

In addition to computational efficiency, several other issues have to be considered when using features from morphological scale-spaces in real-life applications.

Robustness to various artefacts, and mainly noise, should be achieved. Asano and Yokozeki [8] propose the multiresolution pattern spectrum (MPS) to measure size distributions accurately even in the presence of noise in binary images. They suggest to precede each opening by a closing of the same size, so their MPS is nothing more than the Φ^{ASF} feature. Dougherty and Cheng introduced in [28] exterior granulometries to perform recognition of noisy shapes. If the size of the feature set is large (which could be easily observed with 2-D or n-D features), it is necessary to proceed to data or dimension reduction to ensure robustness of the method to the size of the feature set. Naturally statistical approaches such as PCA or MNF may be involved, but one can also rely on genetic algorithms [88]. Moreover, data discretisation may also bring some problems, and robustness against it has to be solved if features with low λ values are analysed. To do so, it is possible to build a new larger and oversampled image from f and to compute morphological features on this image, thus avoiding the problems related to data discretisation [48].

Morphological scale-spaces may require the definition of the underlying SE shape, or the window size and shape when used at a semi-local scale, thus allowing the adaptation of the morphological feature to the data under consideration. Since these parameters have a very strong influence on the resulting features, this is a critical issue. Jan and Hsueh propose to define the window size used with semi-local granulometries using analysis of the global covariance measure [55]. Asano et al [7] propose to define the structuring function which best models a given texture through the use of a pattern spectrum, by first

defining the optimal size of the SE and then determining the appropriate SE values. Balagurunathan and Dougherty [14] deal with the same problem and propose a solution based on a Bayesian framework and dedicated to the binary case.

5 Applications

The different features reviewed in this chapter have been used in the literature to solve various problems. We present here the main areas where they have been applied, as illustrative examples to help the reader to understand the benefit of morphological features over conventional features when dealing with real-life problems.

5.1 Texture segmentation and classification

Since granulometries and pattern spectrum were first proposed to determine the distribution of grains in binary images, the main usage of such morphological features is related to texture analysis, i.e. image segmentation and classification based on textural properties. Indeed, morphological features can achieve to describe the shape, size, orientation, and periodicity of ordered textures, and are also relevant to extract some properties of disordered textures [103].

When computed at a local or semi-local scale, morphological features have been used to perform segmentation of textured images. Early work in this field is due to Dougherty et al. [30] who proposed to consider several features (mean and variance of the pattern spectrum, or more generally the granulometric moments) leading to various studies since then. Among them we can cite [34] where area-based filters are considered. A supervised segmentation scheme is proposed in [87] which requires to learn the different textures before applying the segmentation algorithm. For each image in the morphological scale-space, mean and standard deviation are computed with 3 different SE (square, horizontal and vertical line segments) and lead to the identification of the scales which are relevant for texture recognition.

When applied at a global scale, morphological features can allow texture classification. The Brodatz dataset has been extensively used to deal with this problem, e.g. considering hat scale-spaces [53] or comparing between various dimensionality reduction techniques [120].

Micrographs were studied in [39] where a k nearest neighbours (k-NN) classifier is involved to distinguish between various texture classes. The morphological feature here is a 3-D pattern spectrum with various height, width, and greylevel of the structuring function. Similarly, size-intensity morphological measures have been used to qualify granite textures [88], involving also a k-NN classifier and a genetic algorithm to reduce the feature space.

Comparison of different morphological features for texture analysis has also been investigated, for instance in the context of nondestructive and quantitative assessment of stone decay [72], for Brodatz [9] and for Outex [106] texture databases. This last database has also been used in the comparative evaluations made by Aptoula and Lefèvre [5, 4, 6].

5.2 Biomedical imaging

In the field of biomedical imaging, features built from morphological scale-spaces have been successfully involved in the resolution of various problems due to the high importance of the shape information within visible structures. We give here some examples related to medical imaging and biological imaging.

In the field of Ophthalmology, binary images obtained from specular microscopy are analysed by means of granulometric moments either at a global scale [10] or at a semi-local scale [137] to determine the corneal endothelium status. Segmentation of X-ray mammographies is performed in [12] by relying on a clustering algorithm. Each pixel is characterised by some features which consist of the 3 first moments computed on several semi-local granulometric curves obtained using 10 different SE (both flat and non-flat). In [59], shape matching in the context of tumour recognition in medical images is considered. The difference between two shapes is computed at every scale between aligned shapes (i.e. after a spatial registration of the two shapes) and is finally integrated over all scales to give a global

difference measure. The problem of atherosclerotic carotid plaque classification from ultrasound images is tackled in [60]. The greyscale input image is thresholded to generate three binary images isolating the different tissues. The pattern spectrum is then computed both on these binary images and on the initial greylevel image and used as an image feature for a subsequent SVM classifier. Skin lesion images acquired with diffuse reflectance spectroscopic imaging are analysed in [73] through several pattern spectra computed with various SE and SF. Granulometric features are used in [109] to quantify the size of renal lesions from binarised CT scans.

As biology is concerned, Diatom shells are classified using some features computed on scale-spaces built using top-hat operators by reconstruction (i.e. $\Pi^{\tau\rho}$ series) [53] and using size-shape features [114]. In [95], granulometry is used to define accurate parameters in a global image analysis procedure of infected blood cell images. Based on this work, a technique was proposed more recently [94] to segment and classify malaria parasites. Malaria-infected blood slide images are also analysed in [78] with area-based granulometries. In the field of quantitative cytology, scale-spaces computed with openings by reconstruction are used to perform shape description [76]. Histological images of breast tissue are classified using an SVM with size-density features in [138]. In [123], classification of medaka embryo is performed using a neural network fed with pattern spectrum values computed on binary images. Granulometric moments help to count and classify white blood cells in [111]. Granulometry is involved in [135] to determine accurate parameters to separate overlapping cells. Greyscale granulometries and Fourier boundary descriptors are combined in [110] to perform classification of underwater plankton images with a neural network.

5.3 Remote sensing

Morphological features have also been applied to remote sensing, or satellite image analysis.

Interpretation of multispectral images has been elaborated by Aptoula and Lefèvre in [5] with the comparison of various vector ordering schemes for computing the DMP used in a subsequent supervised pixelwise classification. Lefèvre et al. consider in [63] a size-shape pattern spectrum with rectangular SE to determine automatically the optimal parameters for a noise removal step based on an opening, in the context of a morphological approach to building detection in panchromatic remotely-sensed images. The analysis of DEM (Digital Elevation Map) images was performed by Jackway and Deriche [52] using scale-space fingerprints computed in a semi-local way considering circular regions in order to recognise these areas using a predefined set of fingerprint models. Remotely-sensed textures have also been analysed by means of pattern spectrum in [120]. Finally, some works have been done in pixelwise classification of hyperspectral images, e.g. Benediktsson et al. in [22] and Plaza et al. in [85]. The problem of dimensionality reduction has also been tackled [86]. Post-conflict reconstruction assessment has been addressed in [84], and building detection studied in [100]. In [20], operators by partial reconstruction are used as intermediate filters between standard filters and filters by reconstruction.

5.4 Document analysis

Document images also exhibit strong shape properties, that make them a good support for applying morphological features.

A block-based analysis of binary images is performed in [96] where the authors use the 3 first granulometric moments computed with SE of various orientations to build an off-line signature recognition system. A 2-D granulometry with rectangular SE as features (reduced by means of a PCA transform) for classifying several types of documents (images of PDF files) is proposed in [13]. In [49], a pattern spectrum helps to determine an optimal opening filter for background subtraction in a problem related to watermark analysis in document images.

5.5 Content-based image retrieval and categorisation

With new morphological scale-spaces being defined for greyscale and colour images, CBIR starts to be a possible application field of morphological features.

In [79], each colour image is associated to its colour pattern spectrum. Several SE with various orientations are combined by keeping at each scale the maximum value of the pattern spectra. The resulting feature is included in the Monet CBIR system. The COIL-20 dataset has been used for object recognition with several morphological features, such as shape features extracted from hat scale-spaces [54], quantised size-shape 2-D pattern spectra using attribute scale-spaces [114], or the morphological size-intensity feature [62]. In [112], the size-shape pattern spectra [114] is computed on each colour band independently to solve the problem of colour image retrieval.

As far as the image categorisation problem is concerned, we can mention [50] where the problem of automatic video-genre classification (cartoons vs. photographs) is tackled. Several features are involved, among which a pattern spectrum computed with isotropic structuring functions with a 2-D parabolic profile. In [15], the problem of non-photorealistic rendering of colour images is considered and the proposed solution relies on ASF scale-space filters to extract edge maps similar to sketch-like pictures.

5.6 Biometrics and shape recognition

Biometrics is a very topical issue, and mathematical morphology is a possible tool to compute reliable features as long as image data are available.

In [17], some measures are computed from rectangular size distributions to perform silhouette classification in real-time. Silhouettes are also classified with hat scale-spaces in [54]. 2D shape smoothing is performed in [56] based on the scale-space proposed by Chen and Yan [27], by keeping at each scale λ only pixels which appear in both differential series of openings and closing, i.e. Δ^{γ} and Δ^{φ}. Binary shapes are also compared at several scales to perform silhouette matching in [65]. The gender of walking people can be determined by analysing the binary silhouette with entropy of the pattern spectrum [108].

Xiaoqi and Baozong propose the high-order pattern spectrum (computed from difference between union and intersection of successive ASF) as a measure for shape recognition [130]. In [3], the authors explore how the pattern spectrum can be effectively used to perform shape recognition, and they consider binary images representing planes.

In [80], pattern spectrum is used as an appropriate feature to distinguish between lips. For each individual, several colour images are acquired considering the pronunciation of different vowels, and then binarised to highlight the lip which will be further analysed by means of pattern spectrum with square, horizontal and vertical SE. The fingerprints computed from scale-spaces by reconstruction are evaluated as appropriate features for face description in [89]. Soille and Talbot introduce orientation fields [105] by analysing the $\left\{\Pi^{\psi}_{\lambda,\theta}(f)(p)\right\}$ series in each pixel p and scale λ. More precisely, they compute for each pair (p,λ) the main orientation and its strength by looking for maximal and minimal values of the series with various θ angles. These features are finally used to extract fingerprints. An effective smoothing method for footprint images is proposed in [133], which relies on the analysis of the morphological scale-space by reconstruction. Su et al. [107] introduce the topologic spectrum to deal with shoeprint recognition in binary images. They replace the sum of pixels (or object area) by the Euler number as the Lebesgue measure, thus measuring at each scale the number of components versus holes, and similarly to the pattern spectrum consider the differential series instead of the original one.

5.7 Other applications

Beyond the main applications presented above, morphological features have also been used in other domains.

Acton and Mukherjee explore area scale-space to solve various problems in image processing. In [2] they introduce a new fuzzy clustering algorithm based on area scale-space which performs better than standard ones for pixel classification considering various object identification tasks (coins, cells, connecting rod). In [1] they propose a new edge detector relying on the area scale-space and which does not require any threshold. Gimenez and Evans consider the problems of noise reduction and segmentation of colour images using area-based scale-spaces [42]. Noise reduction has been already addressed by Haralick et al. in [45] with the opening spectrum, a morphological alternative to the Wiener filter.

Warning traffic signs are recognised by means of oriented pattern spectrum in [134]. Soilsection images have been analysed in [31, 113] by means of pattern spectra computed either with area-based or more complex connected filters. The process of preparation of electronic ink is considered in [124] where the size distribution of microcapsules is of primary importance to evaluate the ink quality. Thus the proposed method relies on the analysis of granulometric curve obtained with openings by reconstruction. Pattern recognition based on pattern spectrum and neural network is applied to partial discharges in order to evaluate insulation condition of high voltage apparatuses [136].

6 Conclusion

Mathematical morphology is a very powerful framework for nonlinear image processing. When dealing with image description, it has been shown that scale-space representations are of major importance. So in this chapter, we have presented a review of image features computed from morphological scale-spaces, i.e. scale-spaces generated with operators from Mathematical Morphology. In our study, we consider both local (or semi-local) and global features, from the earliest and probably most famous 1-D features such as granulometries, pattern spectra and morphological profiles, to some recent multidimensional features which gather many complementary information in a single feature.

Due to space constraints, we have limited our study to morphological features which are extracted from scale-spaces built using mainly structural morphological operators (i.e. operators relying on a structuring element or function). To be complete, we have to mention several other works which could have been included in this chapter. Wilkinson [128] focuses on attribute filters to build attribute-spaces, which offer several advantages over structural operators (e.g. no need to define a SE, more invariant, more efficient). Ghadiali [38] brings the fuzzy logic framework to the morphological features by introducing a fuzzy pattern spectrum. Soille [104] proposes the self-dual filters which are particularly effective when dealing with objects which are neither the brightest nor the darkest in the image.

Among the works related to morphological scale-spaces which have not been detailed here, we can mention the use of PDE [116, 69], the multiscale connectivities [24, 113], the generalisations with pseudolinear scale spaces [35, 125], adjunction pyramids [43] or an algebraic framework [47], and finally the use of morphological levellings [77].

To conclude, morphological scale-spaces are a particularly relevant option to build robust image features, due to the numerous desired properties of mathematical morphology. Despite their theoretical interest and the very active community in mathematical morphology, their practical use stays however limited, in particular for more recent multidimensional features. With the comprehensive review presented here and the various usage examples which have been given, we hope the readers will understand their benefits in mining of multimedia data.

References

[1] S.T. Acton and D.P. Mukherjee. Image edges from area morphology. In *International Conference on Acoustics, Speech, and Signal Processing*, pages 2239–2242, Istanbul, Turkey, 2000.

[2] S.T. Acton and D.P. Mukherjee. Scale space classification using area morphology. *IEEE Transactions on Image Processing*, 9(4):623–635, April 2000.

[3] V. Anastassopoulos and A.N. Venetsanopoulos. The classification properties of the pecstrum and its use for pattern identification. *Circuits, Systems and Signal Processing*, 10(3):293–326, 1991.

[4] E. Aptoula and S. Lefèvre. Spatial morphological covariance applied to texture classification. In *International Workshop on Multimedia Content Representation, Classification and Security (IWMRCS)*, volume 4105 of *Lecture Notes in Computer Science*, pages 522–529, Istanbul, Turkey, September 2006. Springer-Verlag.

[5] E. Aptoula and S. Lefèvre. A comparative study on multivariate mathematical morphology. *Pattern Recognition*, 40(11):2914–2929, November 2007.

[6] E. Aptoula and S. Lefèvre. On morphological color texture characterization. In *International Symposium on Mathematical Morphology*, pages 153–164, Rio de Janeiro, Brazil, October 2007.

[7] A. Asano, M. Miyagawa, and M. Fujio. Texture modelling by optimal grey scale structuring elements using morphological pattern spectrum. In *IAPR International Conference on Pattern Recognition*, pages 475–478, 2000.

[8] A. Asano and S. Yokozeki. Multiresolution pattern spectrum and its application to optimization of nonlinear filter. In *IEEE International Conference on Image Processing*, pages 387–390, Lausanne, Switzerland, 1996.

[9] G. Ayala, E. Diaz, J. Demingo, and I. Epifanio. Moments of size distributions applied to texture classification. In *International Symposium on Image and Signal Processing and Analysis*, pages 96–100, 2003.

[10] G. Ayala, M.E. Diaz, and L. Martinez-Costa. Granulometric moments and corneal endothelium status. *Pattern Recognition*, 34:1219–1227, 2001.

[11] G. Ayala and J. Domingo. Spatial size distribution: applications to shape and texture analysis. *IEEE Transactions on Pattern Analysis and Machine Intelligence*, 23(12):1430–1442, December 2001.

[12] S. Baeg, S. Batman, E.R. Dougherty, V. Kamat, N.D. Kehtarnavaz, S. Kim, A. Popov, K. Sivakumar, and R. Shah. Unsupervised morphological granulometric texture segmentation of digital mammograms. *Journal of Electronic Imaging*, 8(1):65–73, 1999.

[13] A.D. Bagdanov and M. Worring. Granulometric analysis of document images. In *IAPR International Conference on Pattern Recognition*, pages 468–471, Quebec City, Canada, 2002.

[14] Y. Balagurunathan and E.R. Dougherty. Granulometric parametric estimation for the random boolean model using optimal linear filters and optimal structuring elements. *Pattern Recognition Letters*, 24:283–293, 2003.

[15] J.A. Bangham, S. Gibson, and R. Harvey. The art of scale-space. In *British Machine Vision Conference*, 2003.

[16] J.A. Bangham, P.D. Ling, and R. Harvey. Scale-space from nonlinear filters. *IEEE Transactions on Pattern Analysis and Machine Intelligence*, 18(5):520–528, May 1996.

[17] O. Barnich, S. Jodogne, and M. van Droogenbroeck. Robust analysis of silhouettes by morphological size distributions. In *International Workshop on Advanced Concepts for Intelligent Vision Systems*, volume 4179 of *Lecture Notes in Computer Science*, pages 734–745. Springer-Verlag, 2006.

[18] S. Batman and E.R. Dougherty. Size distribution for multivariate morphological granulometries: texture classification and statistical properties. *Optical Engineering*, 36(5):1518–1529, 1997.

[19] S. Batman, E.R. Dougherty, and F. Sand. Heterogeneous morphological granulometries. *Pattern Recognition*, 33:1047–1057, 2000.

[20] R. Bellens, L. Martinez-Fonte, S. Gautama, J. Chan, and F. Canters. Potential problems with using reconstruction in morphological profiles for classification of remote sensing images from urban areas. In *IEEE International Geosciences and Remote Sensing Symposium*, pages 2698–2701, 2007.

[21] J.A. Benediktsson, M. Pesaresi, and K. Arnason. Classification and feature extraction for remote sensing images from urban areas based on morphological transformations. *IEEE Transactions on Geoscience and Remote Sensing*, 41(9):1940–1949, September 2003.

[22] J.A. Benediktsson, M. Pesaresi, and K. Arnason. Classification of hyperspectral data from urban areas based on extended morphological profiles. *IEEE Transactions on Geoscience and Remote Sensing*, 43(3):480–491, March 2005.

[23] J.H. Bosworth and S.T. Acton. Morphological scale-space in image processing. *IEEE International Conference on Digital Signal Processing*, 13:338–367, 2003.

[24] U. Braga-Neto and J. Goutsias. Constructing multiscale connectivities. *Computer Vision and Image Understanding*, 99:126–150, 2005.

[25] E.J. Breen and R. Jones. Attribute openings, thinnings, and granulometries. *Computer Vision and Image Understanding*, 64(3):377–389, November 1996.

[26] J. Chanussot, J.A. Benediktsson, and M. Pesaresi. On the use of morphological alternated sequential filters for the classification of remote sensing images from urban areas. In *IEEE International Geosciences and Remote Sensing Symposium*, Toulouse, France, 2003.

[27] M.H. Chen and P.F. Yan. A multiscale approach based on morphological filtering. *IEEE Transactions on Pattern Analysis and Machine Intelligence*, 11(7):694–700, July 1989.

[28] E.R. Dougherty and Y. Cheng. Morphological pattern-spectrum classification of noisy shapes: exterior granulometries. *Pattern Recognition*, 28(1):81–98, 1995.

[29] E.R. Dougherty, J.T. Newell, and J.B. Pelz. Morphological texture-based maximum-likelihood pixel classification based on local granulometric moments. *Pattern Recognition*, 25(10):1181–1198, October 1992.

[30] E.R. Dougherty, J.B. Pelz, F. Sand, and A. Lent. Morphological image segmentation by local granulometric size distributions. *Journal of Electronic Imaging*, 1:46–60, 1992.

[31] A. Doulamis, N. Doulamis, and P. Maragos. Generalized multiscale connected operators with applications to granulometric image analysis. In *IEEE International Conference on Image Processing*, pages 684–687, 2001.

[32] R. Duits, L. Florack, J. De Graaf, and B. ter Haar Romeny. On the axioms of scale space theory. *Journal of Mathematical Imaging and Vision*, 20:267–298, 2004.

[33] E.A. Engbers, R. van den Boomgaard, and A.W.M. Smeulders. Decomposition of separable concave structuring functions. *Journal of Mathematical Imaging and Vision*, 15:181–195, 2001.

[34] N.D. Fletcher and A.N. Evans. Texture segmentation using area morphology local granulometries. In *International Symposium on Mathematical Morphology*, pages 367–376, 2005.

[35] L. Florack. Non-linear scale-spaces isomorphic to the linear case with applications to scalar, vector, and multispectral images. *International Journal of Computer Vision*, 42(1/2):39–53, 2001.

[36] C. Fredembach and G. Finlayson. The 1.5d sieve algorithm. *Pattern Recognition Letters*, 29:629–636, 2008.

[37] V.M. Gadre and R.K. Patney. Multiparametric multiscale filtering, multiparametric granulometries and the associated pattern spectra. In *IEEE International Symposium on Circuits and Systems*, pages 1513–1516, 1992.

[38] M. Ghadiali, J.C.H. Poon, and W.C. Siu. Fuzzy pattern spectrum as texture descriptor. *IEE Electronic Letters*, 32(19):1772–1773, September 1996.

[39] D. Ghosh and D.C. Tou Wei. Material classification using morphological pattern spectrum for extracting textural features from material micrographs. In *Asian Conference on Computer Vision*, volume 3852 of *Lecture Notes in Computer Science*, pages 623–632. Springer-Verlag, 2006.

[40] P. Ghosh and B. Chanda. Bi-variate pattern spectrum. In *International Symposium on Computer Graphics, Image Processing and Vision*, pages 476–483, Rio de Janeiro, October 1998.

[41] P. Ghosh, B. Chanda, and P. Mali. Fast algorithm for sequential machine to compute pattern spectrum via city-block distance transform. *Information Sciences*, 124:193–217, 2000.

[42] D. Gimenez and A.N. Evans. An evaluation of area morphology scale-space for colour images. *Computer Vision and Image Understanding*, 110:32–42, 2008.

[43] J. Goutsias and H.J.A.M. Heijmans. Nonlinear multiresolution signal decomposition schemes. Part I: Morphological pyramids. *IEEE Transactions on Image Processing*, 9(11):1862–1876, November 2000.

[44] E. Hadjidemetriou, M.D. Grossberg, and S.K. Nayar. Multiresolution histograms and their use in recognition. *IEEE Transactions on Pattern Analysis and Machine Intelligence*, 26(7):831–847, July 2004.

[45] R.M. Haralick, P.L. Katz, and E.R. Dougherty. Model-based morphology: the opening spectrum. *Computer Vision, Graphics and Image Processing: Graphical Models and Image Processing*, 57(1):1–12, January 1995.

[46] R.F. Hashimoto and J. Barrera. A greedy algorithm for decomposing convex structuring elements. *Journal of Mathematical Imaging and Vision*, 18:269–289, 2003.

[47] H.J.A.M. Heijmans and R. van den Boomgaard. Algebraic framework for linear and morphological scale-spaces. *Journal of Visual Communication and Image Representation*, 13:269–301, 2002.

[48] C.L. Luengo Hendriks, G.M.P. van Kempen, and L.J. van Vliet. Improving the accuracy of isotropic granulometries. *Pattern Recognition Letters*, 28:865–872, 2007.

[49] H. Hiary and K. Ng. A system for segmenting and extracting paper-based watermark designs. *International Journal of Document Libraries*, 6:351–361, 2007.

[50] T.I. Ianeva, A.P. de Vries, and H. Rohrig. Detecting cartoons: a case study in automatic video-genre classification. In *IEEE International Conference on Multimedia and Expo*, pages 449–452, 2003.

[51] P.T. Jackway. Morphological scale-space. In *IAPR International Conference on Pattern Recognition*, pages C:252–255, 1992.

[52] P.T. Jackway and M. Deriche. Scale-space properties of the multiscale morphological dilation-erosion. *IEEE Transactions on Pattern Analysis and Machine Intelligence*, 18(1):38–51, January 1996.

[53] A.C. Jalba, M.H.F. Wilkinson, and J.B.T.M. Roerdink. Morphological hat-transform scale spaces and their use in pattern classification. *Pattern Recognition*, 37(5):901–915, May 2004.

[54] A.C. Jalba, M.H.F. Wilkinson, and J.B.T.M. Roerdink. Shape representation and recognition through morphological curvature scale spaces. *IEEE Transactions on Image Processing*, 15(2):331–341, 2006.

[55] S.R. Jan and Y.C. Hsueh. Window-size determination for granulometric structural texture classification. *Pattern Recognition Letters*, 19:439–446, 1998.

[56] B.K. Jang and R.T. Chin. Morphological scale space for 2d shape smoothing. *Computer Vision and Image Understanding*, 70(2):121–141, May 1998.

[57] D.G. Jones and P.T. Jackway. Granolds: a novel texture representation. *Pattern Recognition*, 33:1033–1045, 2000.

[58] R. Jones and P. Soille. Periodic lines: definitions, cascades, and application to granulometries. *Pattern Recognition Letters*, 17:1057–1063, 1996.

[59] P. Korn, N. Sidiropoulos, C. Faloutsos, E. Siegel, and Z. Protopapas. Fast and effective retrieval of medical tumor shapes. *IEEE Transactions on Knowledge and Data Engineering*, 10(6):889–904, 1998.

[60] E. Kyriacou, M.S. Pattichis, C.S. Pattichis, A. Mavrommatis, C.I. Christodoulou, S. Kakkos, and A. Nicolaides. Classification of atherosclerotic carotid plaques using morphological analysis on ultrasound images. *Applied Intelligence*, online first, 2008.

[61] A. Ledda and W. Philips. Majority ordering and the morphological pattern spectrum. In *International Workshop on Advanced Concepts for Intelligent Vision Systems*, volume 3708 of *Lecture Notes in Computer Science*, pages 356–363. Springer-Verlag, 2005.

[62] S. Lefèvre. Extending morphological signatures for visual pattern recognition. In *IAPR International Workshop on Pattern Recognition in Information Systems*, pages 79–88, Madeira, Portugal, June 2007.

[63] S. Lefèvre, J. Weber, and D. Sheeren. Automatic building extraction in VHR images using advanced morphological operators. In *IEEE/ISPRS Joint Workshop on Remote Sensing and Data Fusion over Urban Areas*, Paris, France, April 2007.

[64] W. Li, V. Haese-Coat, and J. Ronsin. Residues of morphological filtering by reconstruction for texture classification. *Pattern Recognition*, 30(7):1081–1093, 1997.

[65] Y. Li, S. Ma, and H. Lu. A multi-scale morphological method for human posture recognition. In *International Conference on Automatic Face and Gesture Recognition*, pages 56–61, 1998.

[66] R.A. Lotufo and E. Trettel. Integrating size information into intensity histogram. In *International Symposium on Mathematical Morphology*, pages 281–288, Atlanta, USA, 1996.

[67] B.S. Manjunath, P. Salembier, and T. Sikora. *Introduction to MPEG-7: Multimedia Content Description Interface*. Wiley, 2002.

[68] P. Maragos. Pattern spectrum and multiscale shape representation. *IEEE Transactions on Pattern Analysis and Machine Intelligence*, 11(7):701–716, July 1989.

[69] P. Maragos. Algebraic and pde approaches for lattice scale-spaces with global constraints. *International Journal of Computer Vision*, 52(2/3):121–137, 2003.

[70] G. Matheron. *Random sets and integral geometry*. Wiley, New York, 1975.

[71] G. Matsopoulos and S. Marshall. A new morphological scale space operator. In *IEE Conference on Image Processing and its Applications*, pages 246–249, 1992.

[72] A. Mauricio and C. Figueirdo. Texture analysis of grey-tone images by mathematical morphology: a non-destructive tool for the quantitative assessment of stone decay. *Mathematical Geology*, 32(5):619–642, 2000.

[73] M. Mehrubeoglu, N. Kehtarnavaz, G. Marquez, and L.V. Wang. Characterization of skin lesion texture in diffuse reflectance spectroscopic images. In *IEEE Southwest Symposium on Image Analysis and Interpretation*, pages 146–150, 2000.

[74] A. Meijster and M.H.F. Wilkinson. A comparison of algorithms for connected set openings and closings. *IEEE Transactions on Pattern Analysis and Machine Intelligence*, 24(4):484–494, April 2002.

[75] B.G. Mertzios and K. Tsirikolias. Coordinate logic filters and their applications in image recognition and pattern recognition. *Circuits, Systems and Signal Processing*, 17(4):517–538, 1998.

[76] V. Metzler, T. Lehmann, H. Bienert, K. Mottahy, and K. Spitzer. Scale-independent shape analysis for quantitative cytology using mathematical morphology. *Computers in Biology and Medicine*, 30:135–151, 2000.

[77] F. Meyer and P. Maragos. Nonlinear scale-space representation with morphological levelings. *Journal of Visual Communication and Image Representation*, 11:245–265, 2000.

[78] K.N.R. Mohana-Rao and A.G. Dempster. Area-granulometry: an improved estimator of size distribution of image objects. *Electronic Letters*, 37(15):950–951, 2001.

[79] N. Nes and M.C. d'Ornellas. Color image texture indexing. In *International Conference on Visual Information and Information Systems*, volume 1614 of *Lecture Notes in Computer Science*, pages 467–474. Springer-Verlag, January 1999.

[80] M. Omata, T. Hamamoto, and S. Hangai. Lip recognition using morphological pattern spectrum. In *International Conference on Audio- and Video-Based Biometric Person Authentication*, volume 2091 of *Lecture Notes in Computer Science*, pages 108–114. Springer-Verlag, 2001.

[81] H. Park and R.T. Chin. Decomposition of arbitrarily shaped morphological structuring elements. *IEEE Transactions on Pattern Analysis and Machine Intelligence*, 17(1):2–15, January 1995.

[82] K.R. Park and C.N. Lee. Scale-space using mathematical morphology. *IEEE Transactions on Pattern Analysis and Machine Intelligence*, 18(11):1121–1126, November 1996.

[83] M. Pesaresi and J.A. Benediktsson. A new approach for the morphological segmentation of high-resolution satellite imagery. *IEEE Transactions on Geoscience and Remote Sensing*, 39(2):309–320, February 2001.

[84] M. Pesaresi and E. Pagot. Post-conflict reconstruction assessment using image morphological profile and fuzzy multicriteria approach on 1-m-resolution satellite data. In *IEEE/ISPRS Joint Workshop on Remote Sensing and Data Fusion over Urban Areas*, 2007.

[85] A. Plaza, P. Martinez, R. Perez, and J. Plaza. A new approach to mixed pixel classification of hyperspectral imagery based on extended morphological profiles. *Pattern Recognition*, 37:1097–1116, 2004.

[86] A. Plaza, J. Plaza, and D. Valencia. Impact of platform heterogeneity on the design of parallel algorithms for morphological processing of high-dimensional image data. *The Journal of Supercomputing*, 40(1):81–107, 2007.

[87] J. Racky and M. Pandit. Automatic generation of morphological opening-closing sequences for texture segmentation. In *IEEE International Conference on Image Processing*, pages 217–221, 1999.

[88] V. Ramos and P. Pina. Exploiting and evolving r^n mathematical morphology feature spaces. In *International Symposium on Mathematical Morphology*, pages 465–474, Paris, France, 2005.

[89] E.A. Rivas-Araiza, J.D. Mendiola-Santibanez, and G. Herrera-Ruiz. Morphological multiscale fingerprints from connected transformations. *Signal Processing*, 88:1125–1133, 2008.

[90] J.F. Rivest. Granulometries and pattern spectra for radar signals. *Signal Processing*, 86:1094–1103, 2006.

[91] C. Ronse. Why mathematical morphology needs complete lattices. *Signal Processing*, 21(2):129–154, October 1990.

[92] C. Ronse. Special issue on mathematical morphology after 40 years. *Journal of Mathematical Imaging and Vision*, 22(2-3), 2005.

[93] C. Ronse, L. Najman, and E. Decencière. Special issue on ISMM 2005. *Image and Vision Computing*, 25(4), 2007.

[94] N.E. Ross, C.J. Pritchard, D.M. Rubin, and A.G. Duse. Automated image processing method for the diagnosis and classification of malaria on thin blood smears. *Medical and Biological Engineering and Computing*, 44(5):427–436, May 2006.

[95] C. Di Ruberto, A. Dempster, S. Khan, and B. Jarra. Analysis of infected blood cells images using morphological operators. *Image and Vision Computing*, 20:133–146, 2002.

[96] R. Sabourin, G. Genest, and F. Prêteux. Off-line signature verification by local granulometric size distributions. *IEEE Transactions on Pattern Analysis and Machine Intelligence*, 19(9):976–988, September 1997.

[97] P. Salembier, A. Oliveras, and L. Garrido. Antiextensive connected operators for image and sequence processing. *IEEE Transactions on Image Processing*, 7(4):555–570, April 1998.

[98] F. Sand and E.R. Dougherty. Robustness of granulometric moments. *Pattern Recognition*, 32:1657–1665, 1999.

[99] J. Serra. *Image Analysis and Mathematical Morphology*. Academic Press, 1982.

[100] A.K. Shackelford, C.H. Davis, and X. Wang. Automated 2-d building footprint extraction from high-resolution satellite multispectral imagery. In *IEEE International Geosciences and Remote Sensing Symposium*, pages 1996–1999, 2004.

[101] F.Y. Shih and Y.T. Wu. Decomposition of binary morphological structuring elements based on genetic algorithms. *Computer Vision and Image Understanding*, 99:291–302, 2005.

[102] K. Sivakumar, M.J. Patel, N. Kehtarnavaz, Y. Balagurunathan, and E.R. Dougherty. A constant-time algorithm for erosions/dilations with applications to morphological texture feature computation. *Journal of Real-Time Imaging*, 6:223–239, 2000.

[103] P. Soille. Morphological texture analysis: an introduction. In *Morphology of Condensed Matter*, volume 600 of *Lecture Notes in Physics*, pages 215–237. Springer-Verlag, 2002.

[104] P. Soille. *Morphological Image Analysis : Principles and Applications*. Springer-Verlag, Berlin, 2003.

[105] P. Soille and H. Talbot. Directional morphological filtering. *IEEE Transactions on Pattern Analysis and Machine Intelligence*, 23(11):1313–1329, November 2001.

[106] P. Southam and R. Harvey. Texture granularities. In *IAPR International Conference on Image Analysis and Processing*, volume 3617 of *Lecture Notes in Computer Science*, pages 304–311. Springer-Verlag, 2005.

[107] H. Su, D. Crookes, and A. Bouridane. Shoeprint image retrieval by topological and pattern spectra. In *International Machine Vision and Image Processing Conference*, pages 15–22, 2007.

[108] K. Sudo, J. Yamato, and A. Tomono. Determining gender of walking people using multiple sensors. In *International Conference on Multisensor fusion and integration for intelligent systems*, pages 641–646, 1996.

[109] R.M. Summers, C.M.L. Agcaoili, M.J. McAuliffe, S.S. Dalal, P.J. Yim, P.L. Choyke, M.M. Walther, and W.M. Linehan. Helical CT of von Hippel-Lindau: semi-automated segmentation of renal lesions. In *IEEE International Conference on Image Processing*, pages 293–296, 2001.

[110] X. Tang. Multiple competitive learning network fusion for object classification. *IEEE Transactions on Systems, Man, and Cybernetics*, 28(4):532–543, 1998.

[111] N. Theera-Umpon and S. Dhompongsa. Morphological granulometric features of nucleus in automatic bone marrow white blood cell classification. *IEEE Transactions on Information Technology in Biomedicine*, 11(3):353–359, May 2007.

[112] F. Tushabe and M.H.F. Wilkinson. Content-based image retrieval using shape-size pattern spectra. In *Cross Language Evaluation Forum 2007 Workshop, ImageClef Track*, Budapest, Hungary, 2007.

[113] C.S. Tzafestas and P. Maragos. Shape connectivity: multiscale analysis and application to generalized granulometries. *Journal of Mathematical Imaging and Vision*, 17:109–129, 2002.

[114] E.R. Urbach, J.B.T.M. Roerdink, and M.H.F. Wilkinson. Connected shape-size pattern spectra for rotation and scale-invariant classification of gray-scale images. *IEEE Transactions on Pattern Analysis and Machine Intelligence*, 29(2):272–285, February 2007.

[115] E.R. Urbach and M.H.F. Wilkinson. Efficient 2-d grayscale morphological transformations with arbitrary flat structuring elements. *IEEE Transactions on Image Processing*, 17(1):1–8, January 2008.

[116] R. van den Boomgaard and A. Smeulders. The morphological structure of images: the differential equations of morphological scale-space. *IEEE Transactions on Pattern Analysis and Machine Intelligence*, 16(11):1101–1113, November 1994.

[117] M. van Droogenbroeck. Algorithms for openings of binary and label images with rectangular structuring elements. In *International Symposium on Mathematical Morphology*, pages 197–207, 2002.

[118] M. van Droogenbroeck and M.J. Buckley. Morphological erosions and openings: fast algorithms based on anchors. *Journal of Mathematical Imaging and Vision*, 22:121–142, 2005.

[119] M. Vanrell and J. Vitria. Optimal 3×3 decomposable disks for morphological transformations. *Image and Vision Computing*, 15:845–854, 1997.

[120] M.L.F. Velloso, T.A.A. Carneiro, and F.J. De Souza. Pattern sepctra for texture segmentation of gray-scale images. In *International Conference on Intelligent Systems Design and Applications*, pages 347–352, 2007.

[121] L. Vincent. Grayscale area openings and closings: their applications and efficient implementation. In *EURASIP Workshop on Mathematical Morphology and its Applications to Signal Processing*, pages 22–27, Barcelona, Spain, 1993.

[122] Luc Vincent. Granulometries and opening trees. *Fundamenta Informaticae*, 41(1-2):57–90, January 2000.

[123] S. Wada, S. Yoshizaki, H. Kondoh, and M. Furutani-Seiki. Efficient neural network classifier of medaka embryo using morphological pattern spectrum. In *International Conference on Neural Networks and Signal Processing*, pages 220–223, 2003.

[124] X. Wang, Y. Li, and Y. Shang. Measurement of microcapsules using morphological operators. In *IEEE International Conference on Signal Processing*, 2006.

[125] M. Welk. Families of generalised morphological scale spaces. In *Scale Space Methods in Computer Vision*, volume 2695 of *Lecture Notes in Computer Science*, pages 770–784. Springer-Verlag, 2003.

[126] M. Werman and S. Peleg. Min-max operators in texture analysis. *IEEE Transactions on Pattern Analysis and Machine Intelligence*, 7(6):730–733, November 1985.

[127] M. H. F. Wilkinson. Generalized pattern spectra sensitive to spatial information. In *IAPR International Conference on Pattern Recognition*, volume 1, pages 21–24, Quebec City, Canada, August 2002.

[128] M.H.F. Wilkinson. Attribute-space connectivity and connected filters. *Image and Vision Computing*, 25:426–435, 2007.

[129] A.P. Witkin. Scale-space filtering. In *International Joint Conference on Artificial Intelligence*, pages 1019–1022, Karlsruhe, Germany, 1983.

[130] Z. Xiaoqi and Y. Baozong. Shape description and recognition using the high order morphological pattern spectrum. *Pattern Recognition*, 28(9):1333–1340, 1995.

[131] X.Zhuang and R.M. Haralick. Morphological structuring element decomposition. *Computer Vision, Graphics and Image Processing*, 35:370–382, 1986.

[132] H.T. Yang and S.J. Lee. Decomposition of morphological structuring elements with integer linear programming. *IEE Proceedings on Vision, Image and Signal Processing*, 152(2):148–154, April 2005.

[133] S. Yang, C. Wang, and X. Wang. Smoothing algorithm based on multi-scale morphological reconstruction for footprint image. In *International Conference on Innovative Computing, Information and Control*, 2007.

[134] Z. Yi, J. Gangyi, and C.T. Yong. Research of oriented pattern spectrum. In *IEEE International Conference on Signal Processing*, 1996.

[135] Y. You and H. Yu. A separating algorithm based on granulometry for overlapping circular cell images. In *International Conference on Intelligent Mechatronics and Automation*, pages 244–248, 2004.

[136] L. Yunpeng, L. Fangcheng, and L. Yanqing. Pattern recognition of partial discharge based on its pattern spectrum. In *International Symposium on Electrical Insulating Materials*, pages 763–766, 2005.

[137] V. Zapater, L. Martinez-Costa, G. Ayala, and J. Domingo. Classifying human endothelial cells based on individual granulometric size distributions. *Image and Vision Computing*, 20:783–791, 2002.

[138] I. Zingman, R. Meir, and R. El-Yaniv. Size-density spectra and their application to image classification. *Pattern Recognition*, 40:3336–3348, 2007.